Palaeogeography, Palaeoclimatology, Palaeoecology 265 (2008) 195–213

Contents lists available at ScienceDirect

Palaeogeography, Palaeoclimatology, Palaeoecology

journal homepage: www.elsevier.com/locate/palaeo

A 35,000 year record of changes in the eastern Indian Ocean offshore Sumatra

Davide S. Murgese [a,b], Patrick De Deckker [a,c,*], Michelle I. Spooner [a,d], Martin Young [a,e]

[a] Department of Earth and Marine Sciences, The Australian National University, Canberra ACT 0200, Australia
[b] SEA Consulting S.r.l, Via Cernaia 27 - 10121 Torino, Italy
[c] Research School of Earth Sciences, The Australian National University, Canberra ACT 0200, Australia
[d] Geoscience Australia, GPO Box 378, Canberra ACT 2601, Australia
[e] CSIRO Petroleum, 11 Julius Avenue, Riverside Corporate Park, North Ryde NSW 2113, Australia

ARTICLE INFO

Article history:
Received 14 March 2008
Received in revised form 31 May 2008
Accepted 2 June 2008

Keywords:
Last glacial maximum
Deep chlorophyll maximum
Barrier layer
Java Upwelling System
Monsoon
Organic carbon
Foraminifera
Dinoflagellates

ABSTRACT

We have examined the upper 276 cm of deep-sea core BAR9403 taken at a water depth of 2034 m offshore the southern portion of Sumatra in the eastern Indian Ocean using several micropalaeontological proxies. Faunal counts and stable isotopes of oxygen and carbon of planktic and benthic foraminifers, as well as floral counts of dinoflagellates were obtained to reconstruct conditions in the oceans over the last 35,000 years. At times, we found that when benthic foraminifers indicate high organic content values at the bottom of the ocean this is not paralleled by high productivity signals at the sea surface, but instead must relate to changes in bottom-water circulation as a result of slower water circulation. The marine isotopic stages [MIS] 3-1 are clearly differentiated by benthic and foraminiferal assemblages as well as dinoflagellates and their cysts. MIS 3 is characterised by a much sharper [than today] thermocline that was closer to the sea surface and by the absence of a low-salinity 'barrier layer' which today results from high monsoonal rains. The absence of the latter persisted during the last glacial period [MIS 2] when bottom circulation must have been reduced and high percentages of organic matter occurred on the sea floor combined with low dissolved-oxygen levels. The deglaciation is marked by a change in salinity at the sea surface as seen by the dinoflagellates and planktic foraminifers and progressive alteration of the thermocline was detected by foraminifers suggesting a less productive deep chlorophyll maximum in contrast with MIS 3 and 2. Monsoonal activity commenced around 15,000 cal years ago and was well established 2000 years later. The Holocene is marked by a significant increase in river discharge to the ocean, pulsed by the delivery of organic matter to the sea floor, despite overall oligotrophic conditions at and near the sea surface induced by a permanent low-salinity cap. We did not identify obvious and persistent upwelling conditions offshore Sumatra for the last 35,000 years.

1. Introduction

1.1. Regional oceanography and climate

The eastern Indian Ocean adjacent to the 2 large Indonesian Islands, Sumatra and Java, displays contrasting seasonal characteristics at the sea surface. In the austral summer [December to February], salinity is rather low (≤32 S) due to the monsoonal activity. Overall, the monthly rainfall on Sumatra and offshore in the Indian Ocean is well over 30 cm per month [see http://www.jisao.washington.edu/data/smi/rss/precipssmirssclimr/jpg] with ensuing huge discharges of river water to the ocean. During that time, the predominant winds are such that the southeast trades, that are prevalent between December and April, will force the Southeast Java Current to flow in the direction of Western Australia, before turning southward to eventually join the Southeast Equatorial Current (Fig. 1). In contrast, during the austral winter, the northwest trade winds that are predominant between June and October cause the Current to run in the opposite direction to the one mentioned above, thus flowing towards the Andaman Sea. This coincides with the "drier" season, but still the Island of Sumatra continues to receive much rainfall. Consequently, salinity at the sea surface increases to 34.2.

During the wet season there is a 'barrier layer' (*sensu* Springtall and Tomczak, 1992) that will have been enhanced near the surface of the ocean and which consists of a 'low salinity cap' that is approximately 50 to 100 m thick. The latter prevents any direct exchange between the atmosphere and the deeper ocean below. Of importance also is the Deep Chlorophyll Maximum [=DCM] which sits below the barrier layer, and which can only be exploited by those members of the plankton that can live in deeper waters. The barrier layer's characteristics are typical of the Indo Pacific Warm Pool [abbreviated herewith to 'Warm Pool'], a body of water that today encompasses the entire Indonesian Archipelago and that extends as far east as the Pacific side of Papua New Guinea, in the south just north of Australia and west to the eastern Andaman Sea. The Warm Pool consistently has surface waters ≥28 °C (Yan et al., 1992) and a low salinity cap due to

* Corresponding author. Research School of Earth Sciences, The Australian National University, Canberra ACT 0200, Australia. Fax: +61 2 6125 5544.
E-mail address: patrick.dedeckker@anu.edu.au (P. De Deckker).

0031-0182/$ – see front matter © 2008 Elsevier B.V. All rights reserved.
doi:10.1016/j.palaeo.2008.06.001

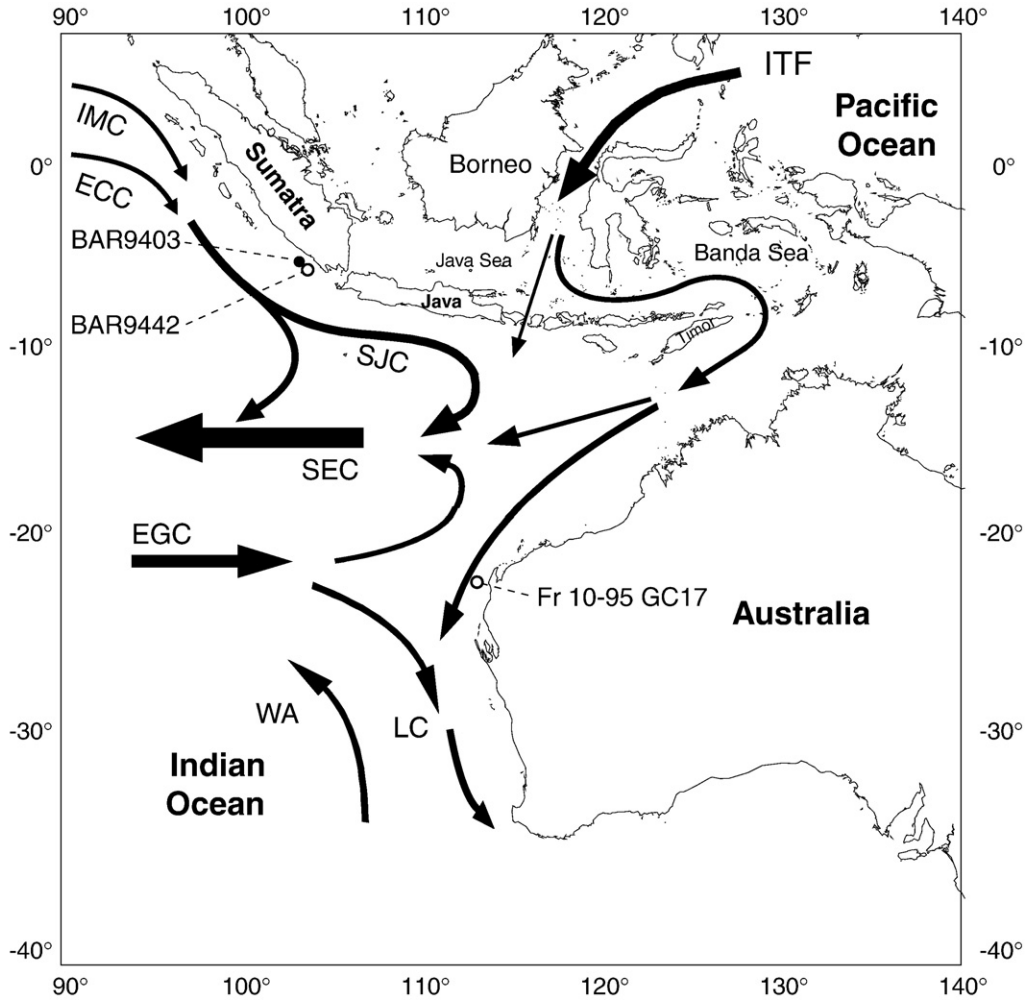

Fig. 1. Map showing the major oceanic current at the surface in the eastern Indian Ocean and the location of the cores mentioned in this paper. Abbreviations: ECC: Equatorial Counter Current; EGC = Eastern Gyral Current; IMC: Indian Monsoon Current; ITF = Indonesian Throughflow; LC = Leeuwin Current; SEC+South Equatorial Current; SJC = South Java Current; WA = West Australian Undercurrent. Currents adapted from Fig. 1 in Wijffels et al. (1996).

the large amount of monsoonal rainfall and fluvial discharges to the sea. Contrasting wind directions, especially over different seasons, can cause some changes to the upper part of the water column, such as a migration of the thermocline, but elsewhere, such as offshore Java, seasonal upwelling can occur, e.g. the Java Upwelling System (see Wyrtki, 1962). Offshore the Island of Sumatra, the thermocline is relatively shallow (~90 m) throughout the year (Levitus, 1998), but no upwelling has been recorded offshore the Island of Sumatra due to the 'barrier layer'.

One critical issue about understanding the interactions between the oceanic atmospheric processes in the Warm Pool region, which plays an important role in global climate (see for review De Deckker et al., 2002), is to determine whether conditions in the atmosphere and surrounding seas have remained the same and, in particular, at a time when the world experienced much colder conditions and significant lower sea levels such as the Last Glacial Maximum, between 23,000 and 19,000 years ago (Yokoyama et al., 2000, 2001; De Deckker and Yokoyama, in press). For this purpose, we have chosen a gravity core taken offshore Sumatra, where today extremely high rainfall is recorded, and where seasonal upwelling is known to operate today. In order to interpret past environmental conditions that span the last 37,000 years of history, we have used a variety of microfossils extracted from the core in order to determine changes through time and identifying conditions, such as those at the sea surface [through foraminifers], at the bottom of the ocean [through benthic foraminifers], and also with respect to salinities at the sea surface and their relationship through river discharges [through the presence of specific dinoflagellates]. The latter will inform us on any major changes in precipitation that may have occurred through time, and this would reflect on past atmospheric conditions. This is rather important as there is still too little information available on hydrological changes that occurred in such an important region that is considered today to be one of the key area supplying 'fresh' water to the global ocean.

1.2. Previous work in the region

De Deckker and Gingele (2002) and Gingele et al. (2002) carried out extensive studies of core BAR9442 which was collected at a depth of 2542 m, some 50 km from the core studied here. These authors described conditions that occurred offshore Sumatra spanning the last 80 ka, but the core suffered from the lack of sufficiently well-preserved calcareous microfossils because of the high abundance of the giant diatom *Ethmodiscus rex* which occurred in many parts of the core. The latter biogenic component prevented obtaining a good chronology based on AMS dates due to the paucity of foraminifera; only a stable isotope chronology could be obtained for that core. Gingele et al. (2002), using clay mineral assemblages, were able to determine changes in monsoonal activity registered by terrigenous input to the sea floor. In particular, these authors demonstrated that

during the glacial period, spanning 70 to 20 ka, strong northeasterly winds associated with the East Asian Winter Monsoon intensified the Indian Monsoon Current and the eastward flowing South Java Current.

1.3. Core bar 9403

The core we have chosen to study is crucially located on the western margin of the Indo-Pacific Warm Pool which, today, is considered to play an important role in the thermohaline circulation of the global ocean, as the waters offshore Sumatra often display low salinities due to heavy monsoonal rains and constantly high (>28 °C) sea-surface temperatures.

2. Materials and methods

2.1. Deep-sea core BAR9403

Piston core BAR9403 was recovered offshore of Sumatra [5° 49.20′ S, 103° 61.90′E] (Fig. 1), west of its southern extremity at a depth of 2034 m. The first 276 cm of this core were sampled every 5 cm. The top 105 cm of the core consist of light yellow clay. Below 105 cm, the sediment consists of greyish olive clay, with some levels (155 cm and 245–255 cm) where the sediment is sandier.

This core is located in an area under the influence of the South Java Upwelling System and, therefore, faunal changes of planktic and benthic foraminifera and dinoflagellates, if related to any variation of the productivity at the sea surface, ought to provide information about modifications of past upwelling intensity/activity.

For the extraction of planktic and benthic foraminifers, approximately 3 cm^3 of each sample was dried in an oven to obtain dry weight. After that, the samples were immersed in a dilute (3%) hydrogen peroxide solution until the clays had fully disaggregated, and the various fractions dried in an oven at 60 °C after being washed with a gentle water jet through a 63 μm.

Sampling for organic-walled dinoflagellate cysts (herein termed 'dinocysts' for the sake of brevity) was carried out at 4 cm intervals throughout the core to a depth of 240–241 cm. The standardized processing procedure for dinocysts is described in detail by de Vernal et al. (1993), and involves dissolution of a known volume of oven-dried sediment with 10% HCl followed by 40% HF. Where necessary, samples were disaggregated by placing them in an ultrasonic bath (<1 min to prevent damaging the cysts), and the remaining residue was then filtered through 120 and 10 μm sieves. Preparation techniques using acetolysis, strong oxidants, alkalis and hot acids were avoided to prevent bias from selective dissolution of the more susceptible cysts.

2.2. Stable isotopes and isotope chronology

The $\delta^{18}O$ record of planktic foraminifera was measured in order to produce an age model for the studied cores, while the $\delta^{13}C$ isotopic signal from the benthic foraminifera was measured in order to acquire information about the deep-water circulation and/or the presence of organic matter at the sea floor.

The species used for isotope analyses were: *Cibidoides wuellerstorfi* for benthic foraminifera, and *Globigerinoides ruber* (white variety) for planktic foraminifera.

C. wuellerstorfi occupies an epifaunal microhabitat (Lutze and Thiel, 1988) and the isotopic composition of its test appears in equilibrium with the TCO_2 of the ambient deep water mass (Duplessy et al., 1984; Altenbach and Sarnthein, 1989). For this reason, the isotopic trend of this species reflects the one characterising the water at the sea floor (Duplessy et al., 1984).

The methodology followed for the preparation of the samples for isotopic analyses is the same for the two types of foraminifera. A number of specimens sufficient to reach the minimum weight of material (180 μg) detectable by the mass spectrometer, were handpicked from each sample from the >250 μm fraction. Specimens were then washed in alcohol and placed in an ultrasonic cleaner for 5 s (up to 10 s when processing benthic foraminifera), in order to eliminate any contaminating residual adhering to the foraminifer test. Oxygen- and carbon-isotopic data obtained are reported in the usual δ notation, which is referred to the PeeDee belemnite (V-PDB) standard. Samples were calibrated against the National Bureau of Standards calcite (NBS-19), assuming values of $\delta^{18}O_{V\text{-}PDB} = -2.20$ ‰ and $\delta^{13}C_{V\text{-}PDB} = -1.95$ ‰.

Analyses were conducted utilising a Finnigan-MAT 251 mass spectrometer at the Research School of Earth Sciences (RSES) at the Australian National University (ANU). The external errors were 0.05‰, for $\delta^{8}O$, and 0.08‰, for $\delta^{3}C$.

2.3. AMS dating of planktic foraminifera

Up to 400 specimens of the planktic foraminifer *G. ruber*, following the common practice followed nowadays by micropalaeontologists to reach good confidence levels with counts, were picked for each level in the core [see Table 1] for AMS chronology conducted at the Australian Nuclear Science and Technology Organisation [=ANSTO]. The foraminifer samples were then placed in a scintillation vial in pure ethanol and allowed to be in an ultrasonic bath for 1 min to clear all disaggregating particles. The clean foraminifers were then washed in milliQ water and then dried. Graphite targets were then made at ANSTO at the ANTARES AMS Facility (see Fink et al., 2004).

The $\delta^{13}C$ values quoted in Table 1 relate solely to the graphite derived from the fraction that was used for the radiocarbon measurement. The data supplied by ANSTO have been rounded according to Stuiver and Polach (1977).

Radiocarbon dates were calibrated using the using the CALIB 5.1 program (Stuiver et al., 2006), and the Marine04 radiocarbon age calibration curve (Hughen et al., 2004). For the oceanic reservoir correction the estimate of the regional ΔR mean for NW Australia and

Table 1
AMS radiocarbon analyses of samples from core BAR9403 showing also calibrated ages

ANSTO codeOZI	Depth in core(cm)	Species analysed	δ13C per mill	Percent Modern Carbo		Conventional 14 C a		Calibrated age BP	
				pMC	1σ error	yr BP	1σ error	yr BP	1σ error
771	0–2	*G. ruber*	−0.3	84.11	0.42	1390	45	889	785–970
772	25–26	*G. ruber*	1.2	46.78	0.22	6105	40	6489	6395–6587
773	55–56	*G. ruber*	1.2	32.92	0.22	8920	60	9553	9448–9653
774	65–66	*G. ruber*	0.9	30.41	0.17	9560	45	10,373	10276–10472
775	100–101	*G. ruber*	0.8	26.62	0.16	10,630	50	11,838	11675–12055
776	125–126	*G. ruber*	0.8	19.38	0.12	13,180	60	15,025	14882–15197
777	155–156	*G. ruber*	2.8	13.17	0.11	16,280	70	19,031	18924–19115
778	185–186	*G. ruber*	2.7	8.35	0.11	19,940	110	23,207	22914–23495
779	205–206	*G. ruber*	-0.4	6.28	0.18	22,230	230	26,174*	
780	265–266	*G. ruber*	0.1	2.2	0.13	30,640	510	35,680*	

* Calibrated age calculated using Bard (1998)'s polynomial.

Java of 67±24 (Bowman, 1985; Southon et al., 2002) was obtained from the CALIB Marine Reservoir Correction Database. All dates reported within this paper are in calibrated radiocarbon years.

For the 2 samples dated in the lower portion of the core (at 205–206 cm and 265–266 cm), the polynomial developed by Bard (1998) was used to calibrate the ages.

2.4. Planktic foraminifers and statistical treatment of the data

Counts of planktic foraminifera were made on splits of the >150 μm fraction to provide a base level for the ecological counts, removing small juvenile and possibly unidentifiable foraminifera. Each sample was split by an Otto-micro splitter until approximately 400 specimens were present in the final split. Planktic foraminifera were identified, at a species level, to reconstruct faunal assemblages through time. The species nomenclature used in this study follows the taxonomy of Saito et al. (1981).

Principal component analysis was conducted on the planktic foraminiferal counts to find ecological groups within the data. The C2 program, version 1.4 (Juggins, 2003) was used to perform the statistical analysis. In accordance with other studies (Martinez et al., 1998), species abundance below 1% was excluded from analysis and raw counts were entered into the program to reduce error.

2.5. Dinoflagellates

Total cyst concentrations (per gram of dry sediment) were calculated as follows:

$$\text{Total cysts/g} = \left[\left(E_{\text{added}} X T_{\text{cysts}}\right)/E_{\text{counted}}\right]/S_{\text{dry weight}}.$$

where E_{added} is the number of exotic spore grains (*Lycopodium* sp.) added to the sample, T_{cysts} is the total number of dinocysts counted in that sample, E_{counted} represents the total number of exotic pollen grains counted in the sample, and $S_{\text{dry weight}}$ is the dry weight of sediment used (in grams). Calculated dinocyst concentrations using the marker-grain method provides an estimate within a standard deviation of 10% for a 0.95 confidence interval (de Vernal et al., 1987; Marret and de Vernal, 1997).

The ratio of heterotrophic (*H*) to autotrophic (*A*) species is calculated as follows:

$$H/A \text{ ratio} = H\text{–cysts}/(H\text{–cysts} + A\text{–cysts}).$$

If selective preservation has not greatly influenced the dinocyst assemblages, the H/A ratio can indicate productivity in the surface waters (e.g., Dale and Fjellså, 1994; van Waveren, 1993; Versteegh, 1994; Cho and Matsuoka, 2001; Roncaglia, 2004), as heterotrophic species (*H*-cysts) are found in high numbers in upwelling regions due to the abundance of suitable nutrients and prey (e.g., diatoms, which are usually the dominant organism in upwelling-related phytoplankton). However, some caution needs to be exercised in using this ratio for productivity purposes, as post-depositional transportation of cysts and selective preservation of species that are sensitive to aerobic decay (e.g. Zonneveld et al., 1997, 2001) can skew the true signature of the *H*/*A* ratio. It is imperative to consider these factors before drawing any conclusions regarding productivity.

2.6. Benthic foraminifera and statistical treatment of the data

Specimens from the >150 μm fraction of each sample were isolated, counted and mounted on micropalaeontological slides. In order to compare the results of the study of benthic foraminifera from the core with the result of the analysis of the core-tops, the absolute number of individuals for each species was converted as the percentage of total foraminifera present in each sample.

Species present with a percentage >2% in at least 1 sample were used for statistical analyses. Similar to the situation observed for the core tops, the specimens belonging to the genera *Fissurina*, *Lagena*, *Lenticulina*, *Oolina* and *Parafissurina* were present in many samples with high species diversity. For this reason, all the species belonging to these genera and used for statistical analysis were grouped together as *Fissurina* spp., *Lagena* spp., *Lenticulina* spp., *Oolina* spp. and *Parafissurina* spp.

The program STATISTICA 6.0 [StatSoft Inc., STATISTICA (data analysis software system), version 6, www.statsoft.com] was used to perform *Q* – mode Factor Analysis (Principal Components) on the species dataset of each core sample.

2.7. Benthic foraminifera accumulation rate (BFAR): applications and problems

A linear relationship between the accumulation rate of benthic foraminifera (BFAR) and the amount of organic matter reaching the sea floor was outlined by Herguera and Berger (1991) and by Herguera and Berger (1994). BFAR has been used worldwide as a proxy to estimate variations of the past carbon-flux rate to the sea floor (Struck, 1995; Thomas et al., 1995; Loubere, 1996; Herguera, 2000; Diester-Haass and Zahn, 2001; Diester-Haass et al., 2002; Rasmussen et al., 2002;). For the eastern Indian Ocean, the selective dissolution of calcareous foraminiferal tests is excluded, as the lysocline is presently indicated at a depth of 2400 m, north of 15°S, and at a depth of 3600 m south of 15°S (Martinez et al., 1998), deeper than the sites studied here. Finally, since the BFAR is a function of the linear sedimentation rate (LSR), this parameter needs to be carefully determined. For the examined cores, LSR was calculated considering AMS measurements (see Section 2.3).

The total number of foraminifera isolated in each sample was used to calculate the benthic foraminifera accumulation rate (BFAR), following the formula proposed by Herguera and Berger (1991):

$$\text{BFAR} = (F)\cdot(\text{LSR})\cdot(\text{DBS})\left[\text{n/cm}^2\text{Kyr}\right];$$

where *F* is the abundance of foraminifera (n/g), LSR is the linear sedimentation rate (cm/kyr) and DBS is the dry bulk sediment (g/cm^3) [g = grams of dry sediment].

3. Results

3.1. Chronology for core BAR9403 based on AMS dates and oxygen isotopes

All the AMS results are presented in Table 1. The oxygen isotope chronology for piston core *BAR9403* is based on the δ^{18}O of *G. ruber* in combination with that of *C. wuellerstorfi* (Fig. 2) with tie points linked to the SPECMAP chronology set by Martinson et al. (1993) and also verified by the AMS dates. The program performing time-series analysis of Paillard et al. (1996) was used to calculate ages for all levels studied in the core. Note that we did not join all the points for the stable isotope analyses done on the benthic foraminifers as some levels had insufficient material for analysis. Nevertheless, the trends are clearly visible and are parallel to those of the planktic foraminifers.

3.2. Planktic foraminifera

A total of 24,374 planktic foraminifer individuals were identified from core BAR9403. The relative abundance of planktic foraminifera shows clear intervals of abundance change paralleling each of the marine isotope stages recorded in core BAR9403 (Fig. 3).

MIS 3 is characterised by *Neogloboquadrina pachyderma* (dextral) recording average abundances of 6%. The relative abundance of *N. pachyderma* (dextral) reduces to <2% near the Last Glacial Maximum [LGM] and does not recover during the Holocene. The

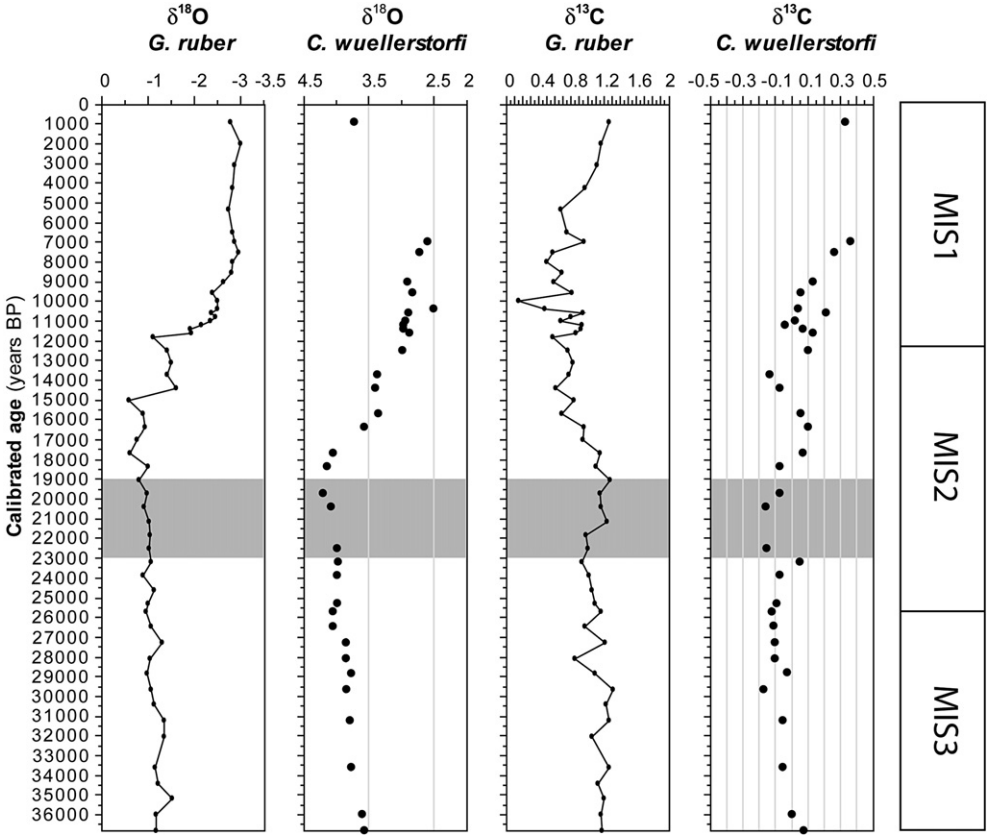

Fig. 2. Chronology of core BAR9403 determined by a combination of the $\delta^{18}O$ composition of planktic and benthic foraminifers and AMS dates done on selected horizons in the core [for more information refer to Table 1 and text]. MIS1-3 refers to the Marine Isotopic Stages 1 to 3. The boundaries between the 3 stages were chosen following the procedures set in Martinson et al., 1993.

occurrence of species *Neogloboquadrina dutertrei* remains fairly stable throughout the entire core but a 5% increase in abundance is seen during MIS 3 and at the Holocene/ MIS 2 transition. *Pulleniatina obliquiloculata* increases in abundance during MIS 3 and the Holocene with abundances >10%, compared to <10% during the LGM. Some minor species, within core BAR9403, only appear during MIS 3 and give further insight into differing conditions in the water column. For example, *Turborotalia quinqueloba* appears in the record with a peak of 2% in relative abundance during MIS 3. Other minor species of deep-water dwellers such as *Globorotalia truncatulinoides* and *Globorotalia crassaformis* also only appear in the record during MIS 3.

The most obvious change in the relative abundance of planktic foraminifera in core BAR9403 is shown by *Globigerina bulloides*. High abundances of *Ga. bulloides* (26%) occur at approximately 12 ka and another peak of abundance (22.7%) occurs during the Holocene. This is compared to the periods from MIS 3 to the LGM where the relative abundance of *Ga. bulloides* is generally <10%. Species *Gr. menardii* also increases its relative abundance from <8% during MIS 3 to peak abundance during MIS 2 of 16% at approximately 14 ka.

Comparatively, periods of increased abundance of *Ga. bulloides* and *Globorotalia menardii* coincide with periods of low abundance for species such as *Gs. ruber* and *Gs. sacculifer*. This is most noticeable after the LGM during the peak relative percentages of *Ga. bulloides* (see Fig. 3). Species *Gs. ruber* records its highest relative abundance of 22.8% during the Holocene but also records a high relative abundance of 20.5% around the 15 ka yr BP. Similarly, species *Gs. sacculifer* records its highest relative abundance of 17% during the Holocene but also records a relatively high percentage (15%) at ~16.5 ka.

3.3. Principal component analysis of planktonic foraminifera

The Eigenvalues of the first five axes from principal component analysis are provided in Table 2. The variance within the species counts of core BAR9403 is explained by each axis, which decreases for each successive axis.

In 56 observations, 28 variables were identified and analysed. The main variance is explained by Component 1 (Eigenvalue 1). However, relatively high variance is explained in the first four components (Fig. 4). Component 1, which explains 32.3% of variance, is dominated with positive scores of *Ga. bulloides*, *Gr. menardii* and *N. dutertrei*. Component 1 is also associated with negative scores from the species *Pulleniatina obliquiloculata, Gs. sacculifer and Gs. ruber*. Component 2, which accounts for 24.4% of the variance in core BAR9403, is dominated by *N. pachyderma* (dextral), *N. dutertrei*, *P. obliquiloculata* and *Globigerinita glutinata*. This component is also associated with strong negative responses by *Ga. bulloides*, *Gs. ruber* and *Gs. sacculifer*. Component 3 accounts for 14.7% of the variance and is dominated by the positive score of *Gt. rubescens* and the strongly negative responses by *Gs. sacculifer*, *N. dutertrei* and *P. obliquiloculata*. Component 4 accounts for 7% variance and is dominated by the high positive species score of *Gs. sacculifer* and also associated with high negative species scores of *Gr. menardii*, *Gs. ruber*, *P. obliquiloculata* and *Gn. glutinata*.

Component plots (bi-plots) were also used to define ecological groups between the first two meaningful components. In the component plots (Fig. 5), the distance between the species relates to the similarity of the species and, therefore, the greater the angle between the vectors the greater the difference between the species. In addition, the vector or line length indicates the importance of the

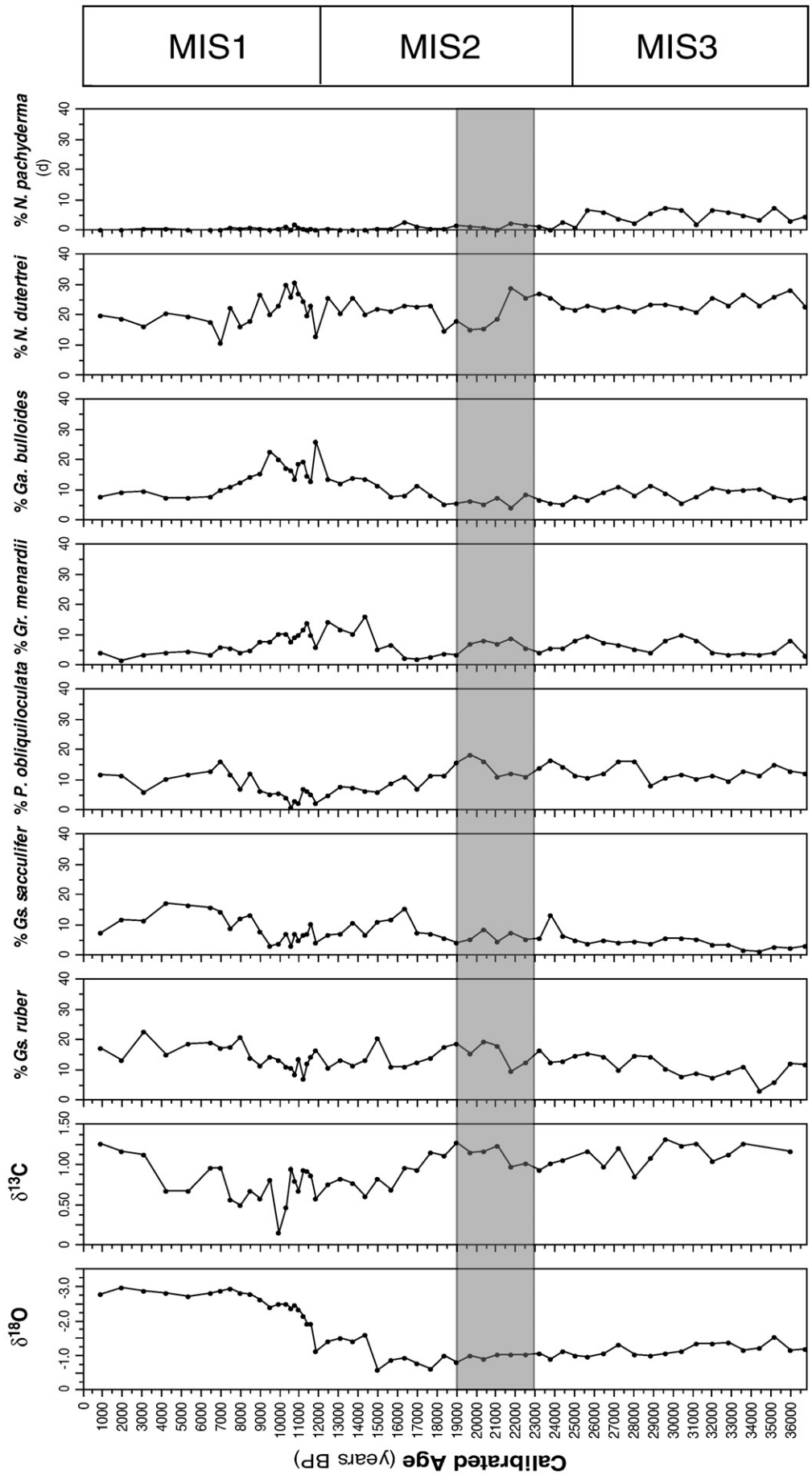

Fig. 3. Composite diagram showing the percentage distribution against time in cal. years BP of the main planktic foraminifer species counted in core BAR9403. The shaded area implies the LGM.

Table 2
Eigenvalues for the first 5 PCA axes carried out on planktic foraminifers from core BAR9403

Axis	Eigenvalue
1	0.323
2	0.244
3	0.147
4	0.07
5	0.063

species in explaining the variance of the species counts. The species scores of the first two components are displayed in the plots above and explain 57% of the variance within core BAR9403 and noted as (1-2) behind the group number.

Group 1 (1-2) consists of species with positive scores in component 1 and 2. *N. dutertrei* is the principal species in Group 1 (1-2). The other primary species *N. pachyderma* (dextral) is separated by a significant angle from *N. dutertrei*, lying close to the Group 1(1-2) and Group 4 (1-2) boundary, thus reducing the correlation between these species (Fig. 4). Group 1(1-2) highest phase of abundance is during MIS 3 and, momentarily, at ~11 ka (see Fig. 3).

Group 2 (1-2) consists of species with positive species scores in the first component but negative scores in the second component. The primary species are *Ga. bulloides* and *Gr. menardii*, with secondary species *Gl. aequilateralis* and *Ga. falconensis*. This group shows an increase of abundance of 25% from ~15 ka to ~6.5 ka as indicated by the relative abundance graph.

Group 3 (1-2) contains species with negative scores in the first and second components. Principal species *Gs. sacculifer* and *Gs. ruber* are highly correlated due to the small angle separating their scores. The secondary species include *Gl. calida* and *O. universa*. The abundance of this group increases after 10 ka.

Group 4 (1-2) contains species with negative scores in the first component and positive scores in the second component. The dominant species is *P. obliquiloculata* and associated with secondary species *Gn. glutinata*, *Gr. truncatulinoides* (dextral), *Gt. rubescens*, *Gt. tenellus*, *Gs. conglobatus*. The sample scores indicate this group dominates during MIS 3 between ~35 ka to 18 ka and increases its abundance again after 9 ka.

3.4. Dinoflagellates

Dinocyst concentrations ranged from between 616 and 12,231 cysts/g for the last ~31 ka in the BAR9403 core, although only 3 horizons recorded concentrations in excess of ~3300 cysts/g (9.5 ka with 8230 cysts/g; 5.3 ka with 11,215 cysts/g, and 0.9 ka with 12,231 cysts/g) (see Figs. 6–7). Twenty-three species of dinoflagellate cysts belonging to the gonyaulacoid (all autotrophic) and protoperidinioid (all heterotrophic) groups were identified in this core, of which *Brigantedinium* and *Spiniferites* dominated.

From 30.8 to 23.9 ka (late MIS 3), concentrations fluctuated between 1489 and 820 cysts/g. Through this interval, the assemblages were dominated by heterotrophic species (predominantly from the genus *Brigantedinium*), with the H/A ratio remaining consistently above 0.57 and ranging up to 0.84.

There is a noticeable decrease in cyst concentrations before the onset of the LGM, from 1489 cysts/g at 26.6 ka, then at the start of the LGM with 1010 cysts/g at 23.9 ka to 674 cysts/g at 22.5 ka. A sudden increase in concentrations occur at 21.8 ka with values more than doubling to 1585 cysts/g. However, concentrations then show a steady and relatively consistent decrease, from 957 cysts/g at ~21.1 ka to ~616 cysts/g at 15 ka, although there are two small peaks at 17.7 ka (930 cysts/g) and 15.7 ka (913 cysts/g). Despite these minor peaks, the concentrations through this period are some of the lowest recovered from the whole core. At the same time, the H/A ratio generally remained between 0.76 and 0.64 for most of this interval. This decreasing trend in cyst concentrations is broken by a threefold increase at ~14.4 ka (1840 cysts/g), with concentrations subsequently staying above ~1400 cysts/g throughout the remainder of the core (see Fig. 8). Relative peaks in cyst concentrations occurs every ~1.6 ka from ~17.7 ka onwards.

O. centrocarpum virtually disappears from the core after ~26.7 ka, being present only at concentrations of <22 cysts/g at 21.1 ka, 19 ka and 17 ka. This species becomes more (relatively) dominant from ~14.4 ka until ~9.9 ka, although it is absent at 11.8 ka and at 11 ka. Concentrations do not increase past 230 cysts/g at any stage, however.

Minor reversals from a heterotrophic-dominated assemblage to an autotrophic one are identified at 19.7 ka (354 cf 495 cysts/g: H/A ratio 0.42), 17 ka (364 cf 380 cysts/g: H/A ratio 0.42) and 13.1 ka (690 cf 842 cysts/g: H/A ratio 0.45). However, autotrophic species (predominantly species of *Spiniferites*) grow frequently more dominant than heterotrophic species from 10.8 ka onwards. The previously unrecorded *Spiniferites* 1 is only present in the upper two samples (5.3 ka and 0.89 ka [core top]) from BAR9403, although concentrations remain low (156 and 117 cysts/g respectively).

3.5. Benthic foraminifers

3.5.1. Factor analysis

Ninety-three benthic foraminifera species were identified among the BAR9403 samples. Mean species percentages ranged between 17.8% (*Bulimina aculeata*) and 0.04% (*Siphogenerina raphanus*). The taxa showing a percentage >2% in at least one sample were selected for *Q-mode* Factor analysis (Principal Components). Factor analysis calculated four varimax factors, which explained 85.35% of the variance of the species distribution. The species scores are listed in Table 3.

The four factors are dominated by four taxa all characterised by high mean percentages. F1 is dominated by *B. aculeata* (43), F2 is dominated by *O. t. umbonatus* (51), F3 is dominated by *Epistominella exigua* (44) and F4 is dominated by *Cibicidoides wuellerstorfi* (53) (number of occurrence is given in brackets) (Fig. 9). Dominant species percentages are shown in Fig. 10. *Oridorsalis tener umbonatus* showed high percentages from 35 to 26 kyr BP (termination of MIS3 – MIS2), while values between 10% and 20% were recorded between 12 and 6 ka (termination of MIS2–late MIS1). *B. aculeata* showed high percentages (>30%) from 26 until 14 ka (MIS2). Between 9 and 4 ka (late MIS1), this species was characterised by percentages ranging between 10% and 20%. *E. exigua* reached percentages >10%, at 35 ka, between 24 and 18.5 ka (early MIS2) and during the last 6 kyr. *C. wuellerstorfi* was characterised by high relative percentage between 14 and 6 ka (termination of MIS2–late MIS1). This taxon reached percentages >10% between 35 and 26 ka (mid MIS3).

3.5.2. Faunal characteristics

Between 35 and 15 ka (MIS3 — termination of MIS2), the agglutinated species percentages were always <5%. They were characterised by high percentages for the last 15 kyr (termination of MIS2–MIS1), between 3% and 14.5%.

Porcellaneous taxa percentages before 27 kyr BP were >15%. Between 27 and 15 kyr BP (mid MIS3–mid MIS2) values decreased, being <15%, and increased again during the last 16 kyr. Infaunal taxa were <40% before 27 ka. Between 27 and 13 ka, percentages were always >50%, with a peak of 68% (at 17 ka). During the last 10 kyr, this group of species displayed percentages <60%, ranging between 28% and 57%.

Diversity indices α, H(S) and E followed similar patterns, steadily increasing from 35 kyr BP to the Present. A major limit can be found at 15 ka: after this point, until the Present, α and E displayed values ranging between 15 and 25; H(S) displayed values generally above 2.7. Dominance (D) showed high values between 25 and 14 ka.

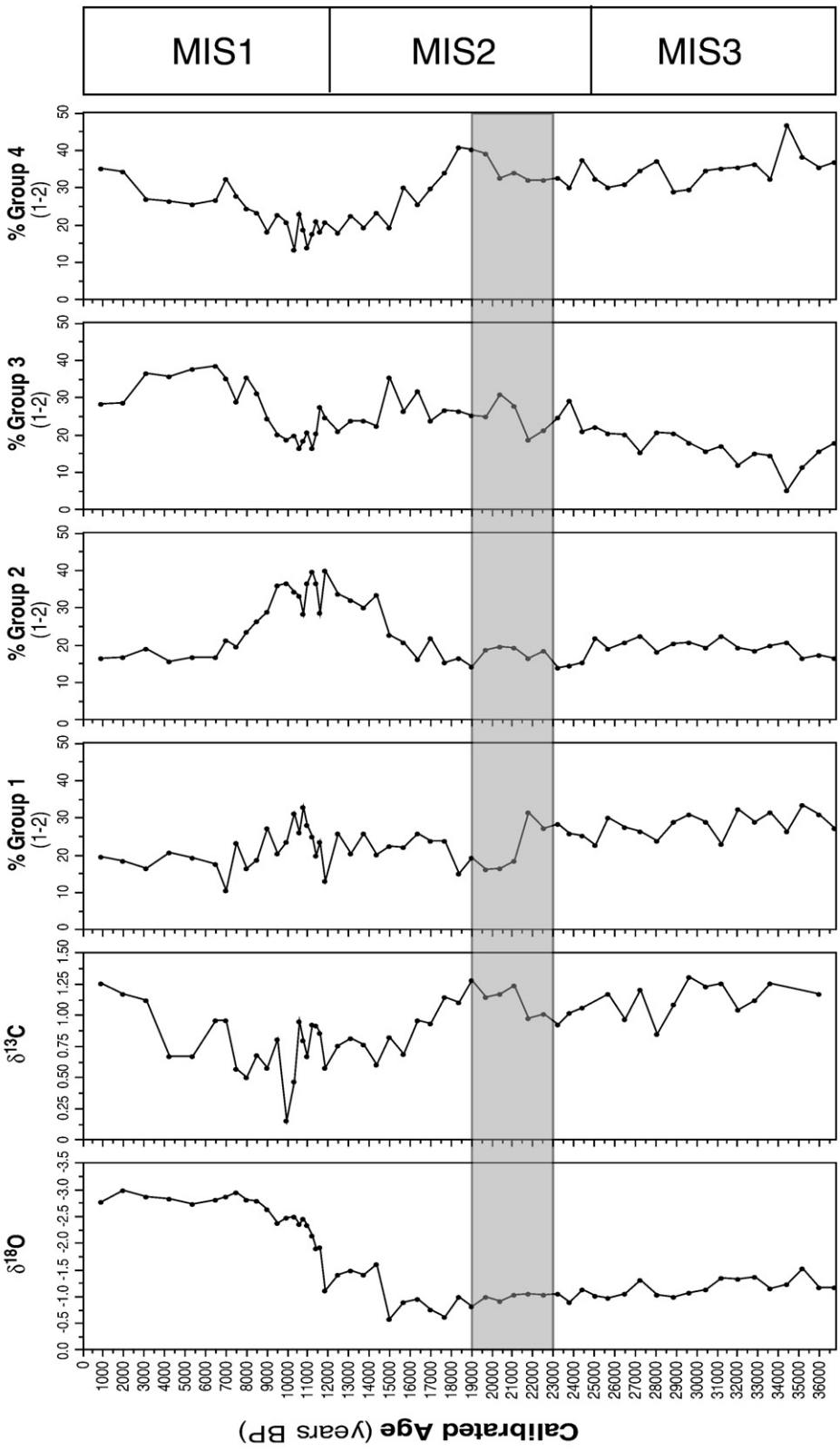

Fig. 4. Plot of the relative abundance of the four groups as found by the principal component analysis of planktic foraminifer from core BAR9403 plotted against the chronology in cal. years BP as well as the stable isotope record for oxygen and carbon obtained on the planktic species *G. ruber*. Note the 3 MIS indicated in the right hand column. The shaded area implies the LGM.

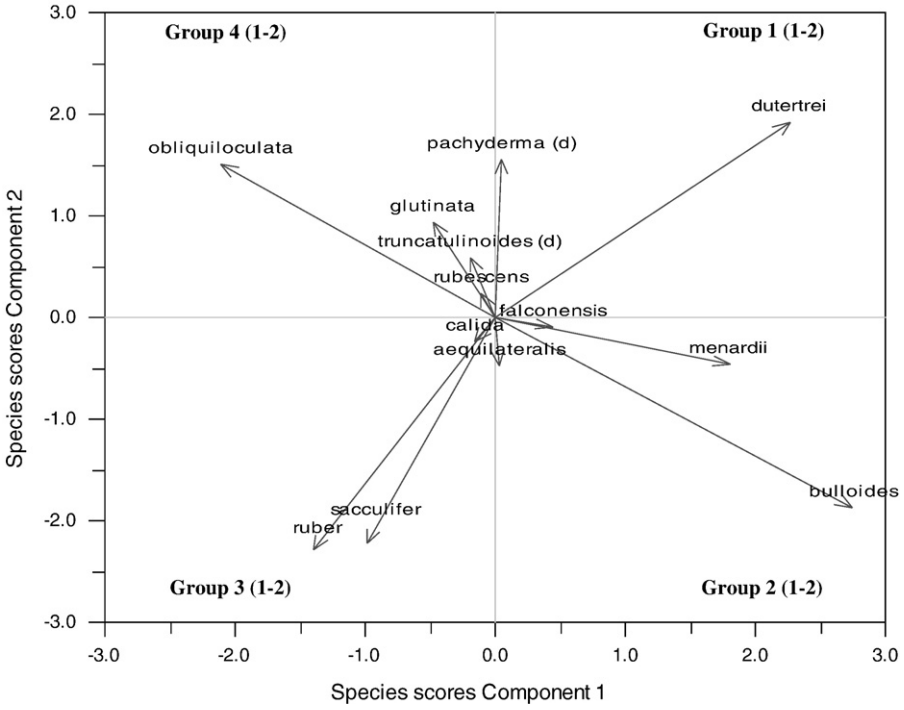

Fig. 5. Bi-plot of Components 1 and 2 for planktic foraminifer counts that explain 58% of the variance in core BAR9403 and which also reveal four ecological groups [see text for more information].

3.5.3. Benthic Foraminifera Accumulation Rate (BFAR) and accumulation rates calculated for B. aculeata, E. exigua and *Uvigerina proboscidea*

The selective destruction of soft-cemented agglutinated foraminifera is instead a phenomenon recorded for the analysed samples, but it only affects a minimal percentage of the total assemblage and should not preclude the use of BFAR.

The BFAR curve (see Fig. 10) showed values ranging between 71 and 240 n/cm^2 kyr^{-1}, for the period between 35 and 29 ka. Between 29 and 14 ka, BFAR was generally higher, reaching values >250 n/cm^2 kyr. After 15 ka, BFAR was characterised by lower values. Between 14 and 10 ka, BFAR decreased passing from 180 to 90 n/cm^2 kyr and between 10 and 6 kyr BP, it ranged between 160 and 53 n/cm^2 kyr. During the last 6 kyr, BFAR decreased, reaching a value of 20 n/cm^2 kyr^{-1} for the Present.

The accumulation rate of *B. aculeata* reached values >30 n/cm^2 kyr^{-1}, between 29 and 14 ka, with a peak of 170 n/cm^2 kyr^{-1} at 22 ka. After 14 ka, this species was nearly absent. A small increase in *B. aculeata* AR was recorded for the last 6 kyr. *E. exigua* was characterised by high AR, between 29 and 14 ka, ranging between 10 and 60 n/cm^2 kyr^{-1}. After 14 ka, the AR of this taxa was nearly 0. It increased again during the last 6 kyr, reaching values >10 n/cm^2 kyr^{-1}. *U. proboscidea* followed a pattern similar to the former two species, although it was characterised by lower AR values compared to the other two taxa. Between 29 and 14 ka, *U. proboscidea* AR ranged between 5 and 20 n/cm^2 kyr^{-1}. After 14 ka, this species displayed AR values <5 n/cm^2 kyr^{-1}, with an isolated peak at 9 ka, when it reached an AR of 15 n/cm^2 kyr^{-1}.

4. Discussion

4.1. Evidence from planktic foraminifers

The distribution of planktic foraminifera in core BAR9403 implies phases of variation within the mixed layer since MIS 3. Overall, MIS 3 appears to be a period of reduced vertical mixing resulting in the stratification of the mixed layer. PCA analysis (see Fig. 5) and the sample scores indicate that Group 1 (1-2), containing species *Neogloboquadrina dutertrei* and *Neogloboquadrina pachyderma*, dominated over the other ecological groups during MIS 3 and momentarily at 11 ka (75 cm). Species *N. dutertrei* and *N. pachyderma* are both considered thermocline dwellers whose increased abundance has been linked to the development of a Deep Chlorophyll Maximum layer (=DCM). A DCM is initiated when the upper water column is stratified and an increase in chlorophyll production occurs at the thermocline (Fairbanks and Weibe, 1980; Thunell and Sautter, 1992), therefore, resulting in optimal conditions for these heterotrophic species.

Cluster analysis by Ding et al. (2006) of core-tops within the Indonesian Archipelago classified the surface waters of the Sumatra Region as being relatively oligotrophic, low in salinity, small in seasonal temperature differences, shallow thermocline and of high dissolution. Ding et al. (2006) revealed that *N. dutertrei* obtained the second highest abundances in the 'Indian Monsoon Sumatra Region' where core BAR9403 is located, due to a shallow thermocline and low salinity waters. In the relative abundance counts in core BAR9403, *N. dutertrei* is the most abundant species throughout the entirety of the core with an increase in abundance of 5% during MIS 3 and 11 ka. However, *N. pachyderma* (d) is not present in Ding et al (2006) core-top counts. The appearance of *N. pachyderma* (d) species during MIS 3 in core BAR9403 indicates a reduction in temperatures at the base of the thermocline compared to the present. High frequencies of *N. pachyderma* are linked to waters with low temperature (10°–14 °C), low salinity (34 and 35.5), and high nutrient (phosphate) levels 1.7 μg at/l (Bé and Hutson, 1977).

It is also shown through the abundances of *Globigerina bulloides* and *Globorotalia menardii,* the principal species of PCA Group 2 (1-2) that upwelling conditions did not occur during MIS 3 (Fig. 3) but, instead, the conditions favoured the development of a DCM layer. Species, *Ga. bulloides* and *Gr. menardii*, are both considered to be 'upwelling' indicators in tropical regions (Bé, 1977; Thunell and Reynolds, 1984; Auras-Schudnagies et al., 1989; Kroon and Nederbragt, 1990; Martinez et al., 1998; Ganssen and Kroon, 2000). Our conclusion relies on the fact that Group 2 (1-2) does not show a

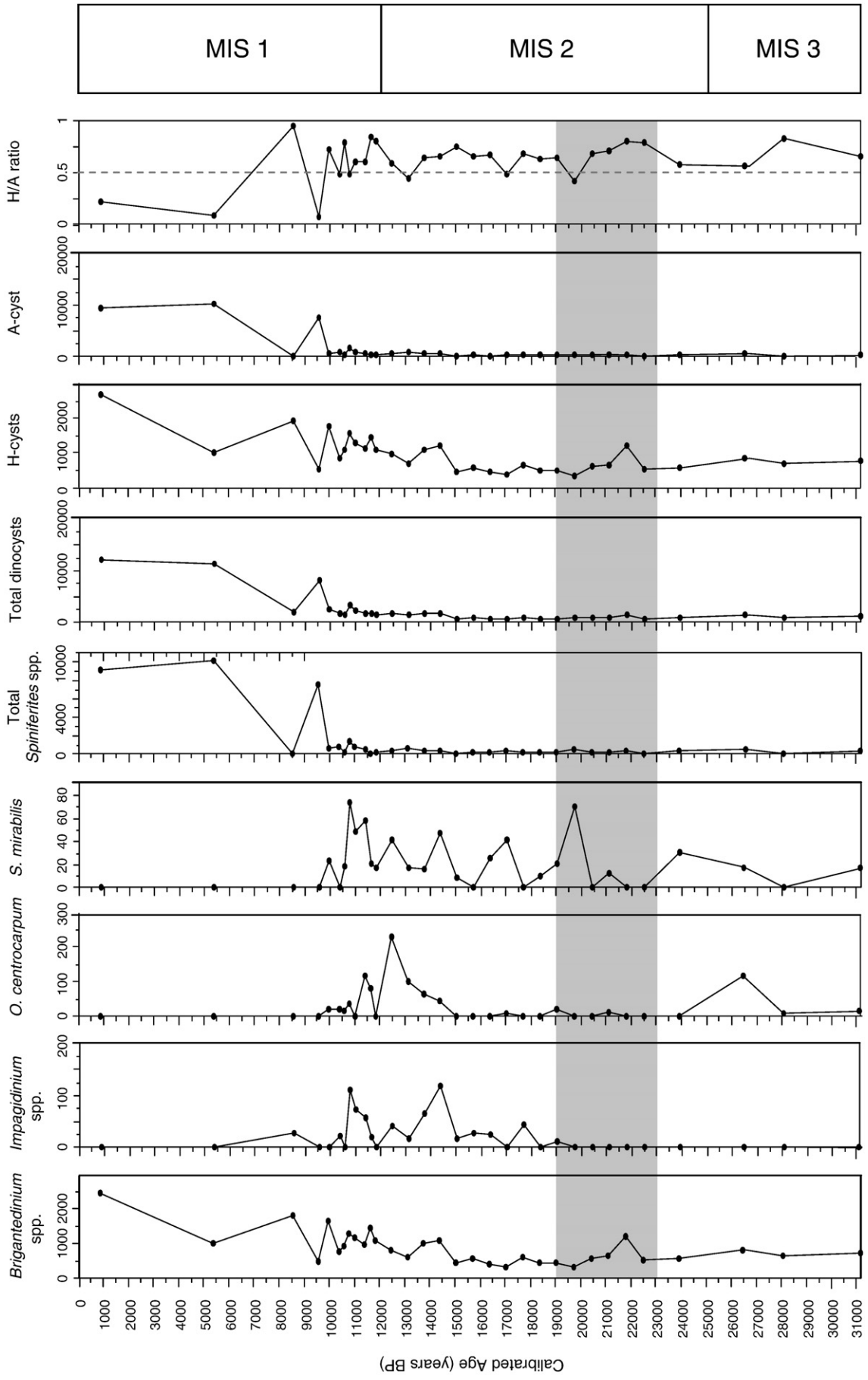

Fig. 6. Plot of the major dinoflagellate species and cysts recovered in core BAR9403 against time in cal. years BP. Note that the distribution of taxa does not extend as far back in time as for the foraminifers in the same core as no dinoflagellates were recovered below 31 ka. The shaded area implies the LGM.

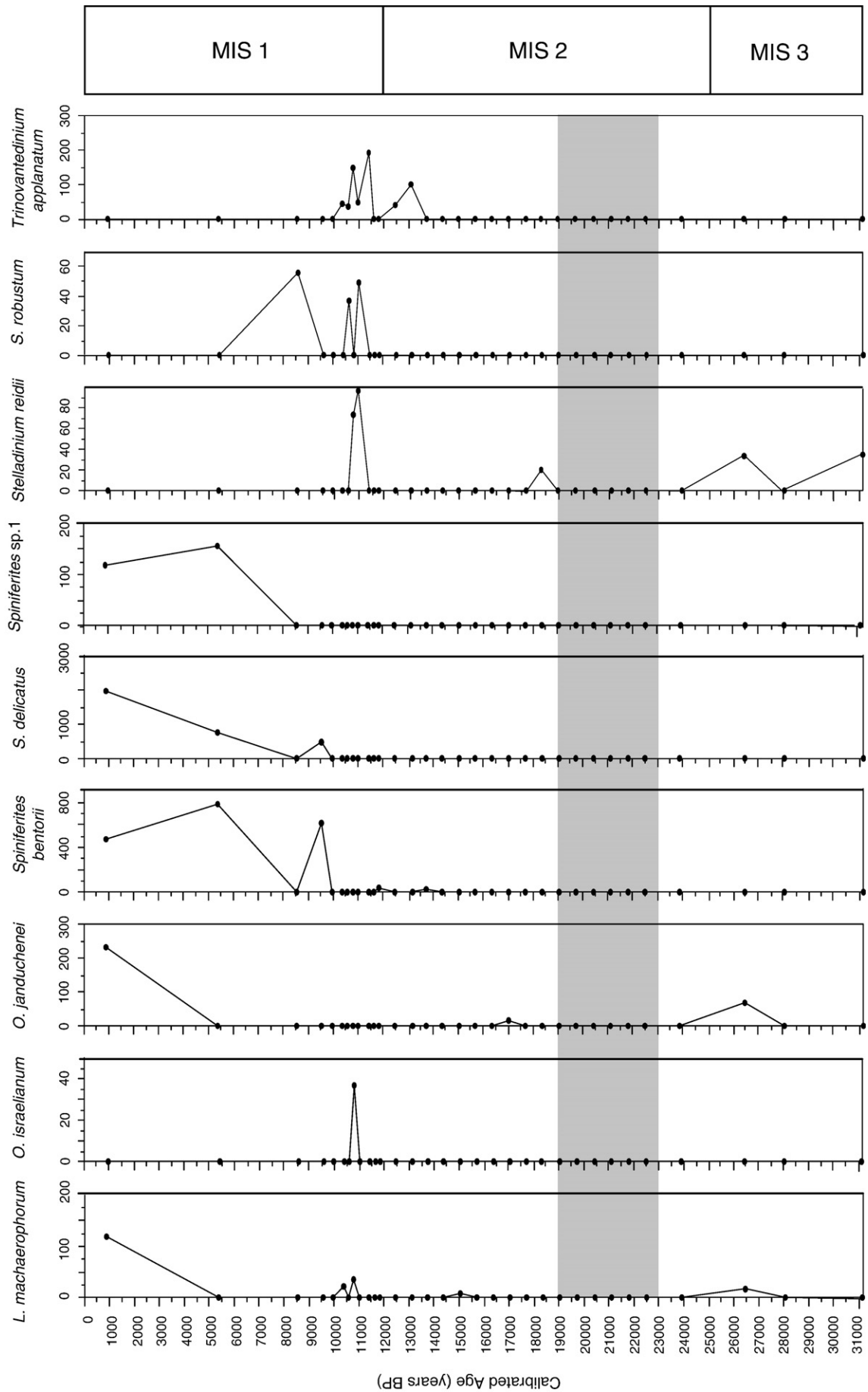

Fig. 7. Plot of the minor dinoflagellate species recovered in core BAR9403 against time in cal. years BP. Note that the distribution of taxa does not extend as far back in time as for the foraminifers in the same core as no dinoflagellates were recovered below 31 ka. The shaded area implies the LGM.

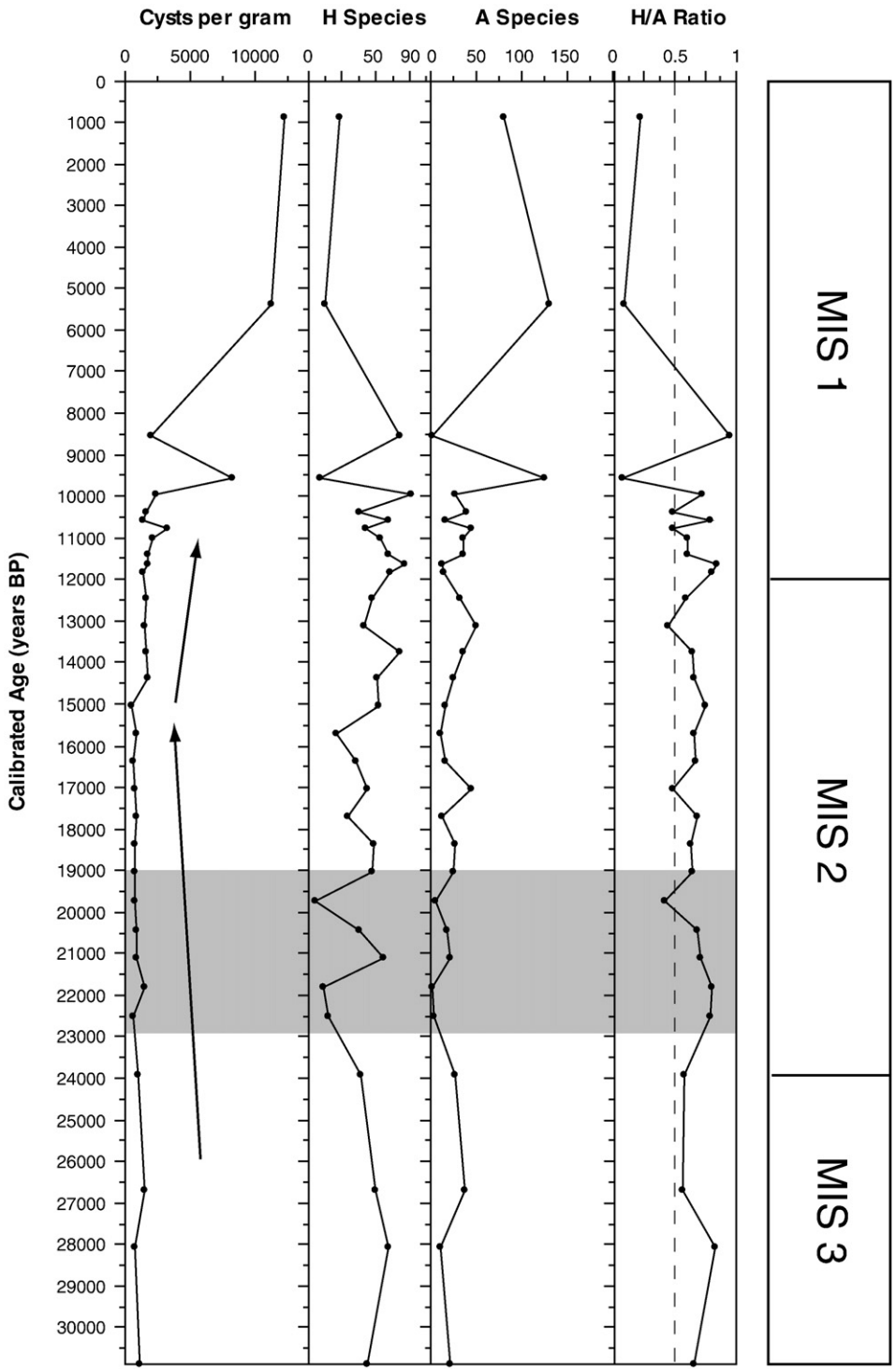

Fig. 8. Plot of autotrophic (A) and heterotrophic (H) dinoflagellate species and the H/A ratio that is used to indicate productivity at the sea surface. The shaded area identifies the LGM.

response to the existence of colder water and possible nutrients at the sea surface during MIS 3 (Fig. 3). This again suggests that the mixed layer was stratified and nutrients did not reach the sea-surface and, therefore, 'upwelling' conditions were not established during MIS 3.

De Deckker and Gingele's (2002) analyses of core BAR9442, located ~50 km from BAR9403, indicated 'blooms' of the "giant" diatom *Ethmodiscus rex* between 28 ka and 19 ka. These authors claim that blooms occur when the water-column is permanently stratified, with a substantial increase in salinity and high levels of silica and nitrate near the sea-surface. This period coincides with the indicated phase of stratification within core BAR9403. In addition, a regional pattern of DCM development was already observed within the various seas of the Throughflow region by Linsley et al. (1985), Barmawidjaja et al. (1993), Ding et al. (2002) and Spooner et al. (2005) for MIS 3 and MIS 2.

The primary species of Group 4 (1-2) is *Pulleniatina obliquiloculata*. The sample scores indicate this group dominates during MIS 3 between ~28 ka to 23 ka and increases its abundance again at ~19 ka. *Pulleniatina obliquiloculata* is predominantly a tropical species and has been associated with warm-water masses such as the South Equatorial Current (Bé and Hutson, 1977) and the Kuroshio Current (Wang et al., 1999; Li et al., 1997).

Table 3
Factor scores of the Q-mode varimax factors in piston core BAR9403

Species	Factor 1	Factor 2	Factor 3	Factor 4
Allomorphina pacifica	−0.3089	−0.1891	−0.1440	−0.4228
Anomalina globulosa	−0.1029	−0.3378	−0.5053	−0.1177
Astrononion echolsi	−0.0757	−0.2354	−0.5619	0.2702
Bolivina robusta	−0.1284	−0.2581	−0.4080	−0.3951
Bolivinita quadrilatera	−0.0449	−0.2518	−0.2155	−0.4513
Brizalina semilineata	−0.2288	−0.2768	−0.3201	−0.3363
Bulimina aculeata	7.2886	0.5376	−1.0540	−0.6130
Bulimina costata	−0.0036	0.8853	0.8493	−0.5370
Bulimina exilis	−0.1731	0.3728	−0.3462	−0.7523
Cassidulina laevigata	0.1427	0.7604	−0.1672	0.1645
Ceratobulimina pacifica	−0.1552	−0.2852	−0.3917	−0.4301
Chilostomella oolina	−0.1833	−0.0229	0.5445	1.1802
Cibicidoides bradyi	−0.1231	−0.2956	−0.1109	0.8635
Cibicidoides pseudoungerianus	−0.1755	−0.4268	−0.3179	0.2755
Cibicidoides robertsonianus	−0.2503	−0.3103	−0.0965	−0.4739
Cibicidoides wuellerstorfi	0.4494	0.0754	−0.0115	5.6760
Eggerella bradyi	−0.1987	−0.3063	−0.0625	−0.3695
Epistominella exigua	0.9489	−1.0216	6.7501	−0.9394
Fissurina sp.	−0.0773	−0.2433	−0.0691	−0.1458
Fursenkoina bradyi	−0.1916	−0.2707	−0.2176	−0.5379
Fursenkoina fusiformis	−0.0744	0.3702	−0.2660	0.2612
Fursenkoina sp.	−0.2311	−0.3101	−0.2070	−0.4578
Gavelinopsis lobatulus	−0.0627	−0.3006	−0.4778	−0.1508
Globobulimina affinis	−0.2283	−0.1015	0.4461	−0.3164
Globobulimina pacifica	−0.2208	−0.3368	0.3832	0.0175
Globocassidulina subglobosa	0.1451	−0.4291	−0.0162	0.7227
Gyroidinoides orbicularis	−0.2249	−0.3363	−0.4198	0.6359
Gyroidinoides polius	−0.2782	−0.3311	0.1473	0.1638
Gyroidinoides soldanii	−0.2196	−0.1538	−0.4720	−0.3148
Hoeglundina elegans	0.2484	0.2048	−0.3849	0.7204
Hyalinea balthica	−0.2711	−0.2094	−0.0404	−0.4843
Karreriella bradyi	−0.2885	−0.2768	−0.0969	−0.3526
Lagena sp.	−0.2595	−0.3551	0.0259	−0.2310
Lenticulina sp.	−0.2639	−0.1505	−0.2030	−0.4846
Loxostomum karrerianum	−0.2686	−0.2785	−0.0740	−0.4608
Melonis barleeanum	−0.4038	0.0621	−0.0222	1.6341
Melonis pompilioides	−0.2687	−0.2924	−0.1615	−0.4811
Miliolinella subrotunda	−0.2506	−0.1645	−0.2867	−0.5811
Nonionella bradyi	−0.2498	−0.1729	−0.3645	−0.4611
Nummoloculina irregularis	−0.2253	−0.1223	−0.3162	−0.5907
Oridorsalis tener umbonatus	−0.6304	7.0328	0.6723	−0.0899
Osangularia cultur	−0.1744	−0.1194	−0.4819	−0.3035
Parafissurina sp.	−0.1627	−0.2137	−0.3682	−0.4435
Pullenia bulloides	−0.2492	−0.3133	0.2096	−0.0141
Pullenia quinqueloba	−0.2011	−0.3257	0.0019	−0.1965
Pyrgo depressa	−0.1689	−0.0409	−0.4007	−0.4149
Pyrgo lucernula	−0.2457	0.0284	−0.4646	−0.6110
Pyrgo murrhina	−0.0549	0.9087	1.6953	0.4588
Pyrgo serrata	−0.1001	−0.1312	−0.3007	−0.5876
Quinqueloculina seminulum	−0.2555	−0.1375	−0.2256	−0.3546
Quinqueloculina venusta	−0.1772	0.7055	−0.3634	−0.8163
Robertinoides brady	−0.1222	−0.2627	−0.3583	−0.5413
Sigmoilopsis schlumbergeri	−0.1801	−0.0502	−0.7339	0.8957
Siphogenerina raphanus	−0.2631	−0.1826	−0.2915	−0.5857
Siphotextularia catenata	−0.2008	−0.0380	−0.3727	−0.5857
Uvigerina peregrina	0.0874	−0.5457	0.8255	1.5660
Uvigerina proboscidea	0.3117	−0.3550	0.5466	2.3568
Valvulinaria araucana	0.2753	−0.1747	0.0729	−0.4287

The species listed in bold are the 4 taxa whose distributions are presented in Fig. 10.

The sample scores reveal that Group 4 (1-2) and Group 1 (1-2) alternate in dominance during MIS 3. Previous studies have linked the abundance of *P. obliquiloculata* to its sensitivity to winter temperatures and, therefore, high concentrations of *P. obliquiloculata* occur during warm winter temperatures at the subsurface (Li et al., 1997; Pflaumann and Jian, 1999). The high relative abundance of *P. obliquiloculata* within Group 4 (1-2) and *N. pachyderma* in Group 1 (1-2) during MIS 3 initially appears to be contradictory but may also support the hypothesis that the water column was stratified during this period. The study by Bé (1977) in the region of core BAR9403 found *P. obliquiloculata* predominantly between 50 and 100 m while *N. pachyderma* was predominantly below 100 m. Either stratification provided temperature niches for both these species or the temperature at the base of the thermocline went through seasonality phases. Alternatively the deepening of the mixed layer into cooler, deeper waters could explain the increased abundance of *N. pachyderma* (d) during MIS 3. Thickening of the mixed layer due to stratification has been observed within the Santa Barbara Basin by Pak and Kennett (2002).

Pulleniatina obliquiloculata is one of the most dissolution-resistant species in the low latitudes and can make up to 70% of the total fauna in the Western Pacific sediments (Thompson, 1981 and Thiede et al., 1997). It is believed that dissolution is not the controlling factor on the abundances of planktic foraminifera in core BAR 9403 due to the lack of etching on the foraminifer tests. In addition, the low relative percentages of other dissolution-resistant species such as *Gr. menardii* during MIS 3 and the Holocene coincide with high abundances of *P. obliquiloculata*.

During MIS 2, the relative abundance of *N. dutertrei* reduced slightly, *N. pachyderma* relative abundance reduced to < 1% and the low abundance of upwelling species such as *Ga. bulloides* was maintained from MIS 3 to MIS 2 (see Fig. 3). The PCA analysis grouped *Gs. ruber* and *Gs. sacculifer* together and the sample scores indicated that Group 3 (1-2) dominated over the other PCA groups during the LGM and the Holocene. From these results the LGM appears to be characterised by the abundance of tropical-subtropical species with a preference for oligotrophic conditions. In addition, the higher abundance of these tropical-subtropical species suggests the water column was still stratified and nutrients may not have been entrained into the upper surface layer through wind-forced mixing which occurs presently (Sprintall et al., 2002).

The major change registered in core BAR9403 is around the upwelling signal of PCA Group 2 (1-2) containing *Ga. bulloides* and *Gr. menardii*. The sample scores indicate that this group dominated from 14 ka to 9 ka (Fig. 3). Consequently, we interpret this phenomenon to indicate that nutrients were upwelled to the sea-surface for that time period. The abundance of Group 3 (1-2) and Group 4 (1-2) was also reduced from 15 ka to 9 ka and this implies the removal of the stratified structure of the water column. At the LGM-Holocene transition, De Deckker and Gingele (2002) recorded a high Ba_{excess}, and low *E rex* abundance in core BAR9442 and suggested the removal of stratified conditions and this further supports our interpretation for the region.

Presently, upwelling along the coast of Java operates during the SE Monsoon as a result of southward Ekman transport (Wyrtki, 1962) but nutrients do not reach the surface due to an increase in the transport of the Throughflow (Bray et al., 1997). Martinez et al. (1998) showed that the change in abundance of species, such as *N. pachyderma*, *N. dutertrei* and *Ga. bulloides*, varies around the region and depend on mixed layer thickness and the intensity of the Java Upwelling System. A more dynamic and productive Java Upwelling System encouraged by the SE Monsoon during the LGM is indicated in studies by Martinez et al. (1999), Takahashi and Okada (2000), Gingele et al. (2001) and Gingele et al. (2002). In addition, palaeoproductivity proxy investigations by Müller and Opdyke (2000) in the Timor passage indicate increased nutrients in the mixed layer during MIS 2. However, results from cores BAR9403 and BAR9442 off the coast of Sumatra suggest that upwelling did not occur until after the LGM. It is possible the upwelling signal in core BAR9403 is evidence of a more intense Java Upwelling System and hence monsoonal system from 14 ka.

4.2. Evidence from dinoflagellates

4.2.1. Possible influences upon cyst assemblages

Before any worthwhile interpretation of the dinocyst fossil record from BAR9403 can be made, it is imperative that post-depositional processes such as transportation, selective decay and dissolution are considered, as these factors can create a biased view of the actual thanatocoenosis. We believe that the effect of sea level changes through time did not affect the abundance of dinoflagellate cysts *per se* as there was little change of the coast line with respect to the core

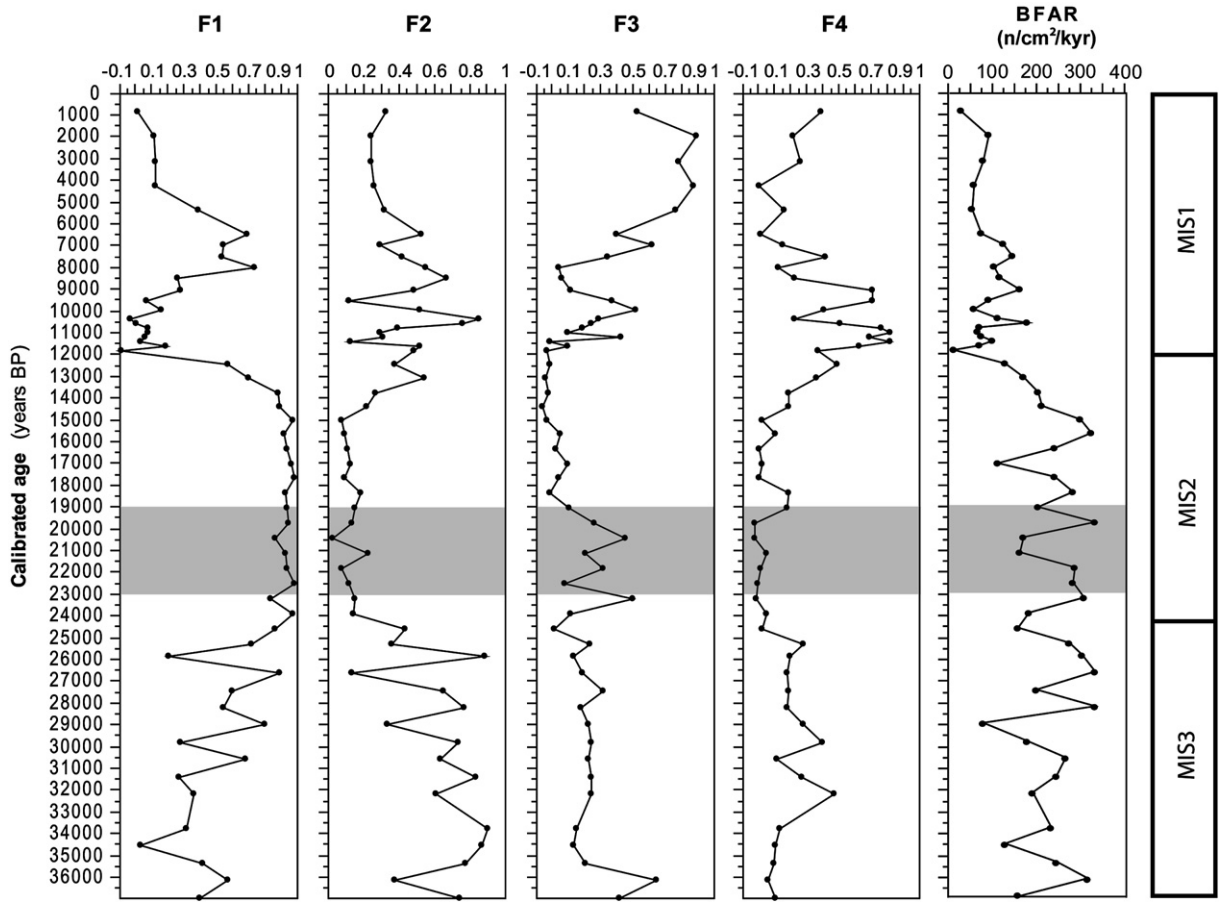

Fig. 9. Distribution of the 4 major factor loadings for the benthic foraminifers from core BAR9403 plotted against the chronology in cal. years BP. Note that 2 additional samples were examined for levels older than 35.5 k years BP in contrast with the planktic foraminifers. The shaded area implies the LGM.

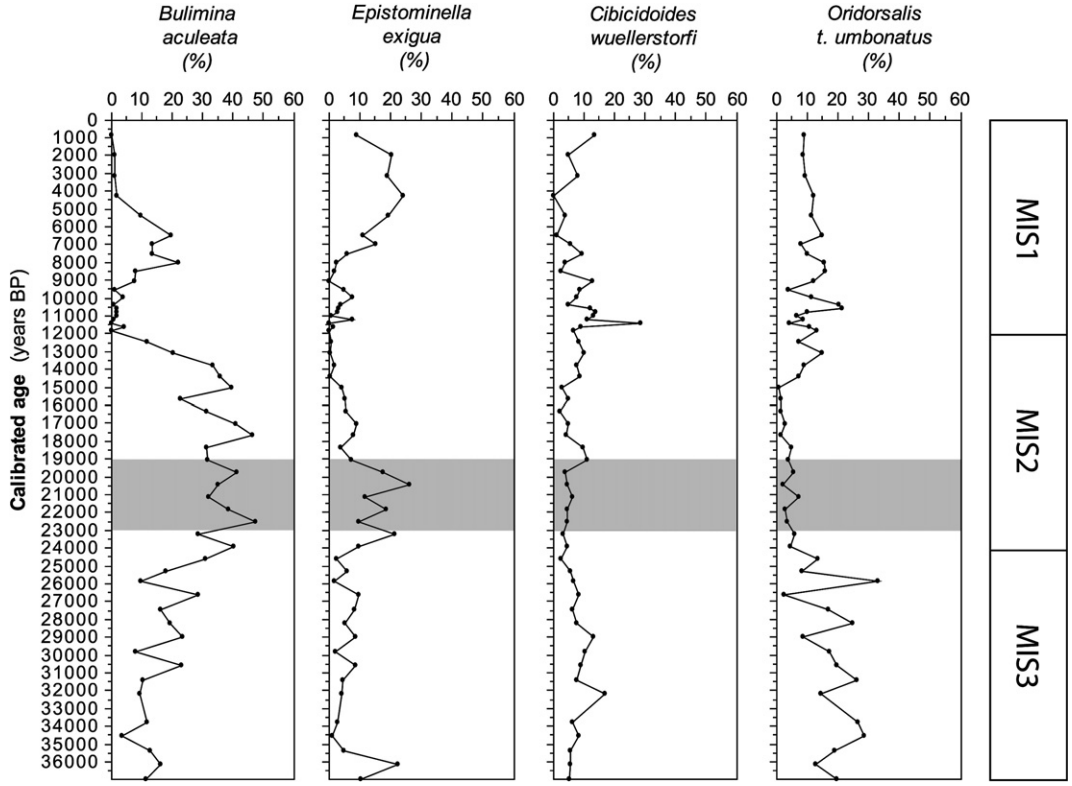

Fig. 10. Percentage distribution of the four principal benthic foraminifer taxa recovered in core BAR9403 against time in cal. years BP. Note that 2 additional samples were examined for levels older than 35.5 k years BP in contrast with the planktic foraminifers. The shaded area implies the LGM.

site and proximity to the land was not much different between periods of low sea level [eg at the LGM] and today.

4.2.1.1. Transportation effects. High river runoff results in an annual sediment discharge off the western coast of Sumatra into the Indian Ocean of approximately 284×10^6 10^6 t/yr, with 498×10^6 10^6 t/yr discharged off the eastern coast of Sumatra into the southern South China Sea (Milliman et al., 1999). These values are some of the highest of all the Indonesian islands. By comparison, Java has a discharge volume of 109×10^6 10^6 t/yr into the Indian Ocean, while Timor has 59×10^6 10^6 t/yr (Milliman et al., 1999).

Species diversity increases up-core through BAR-9403, with the coastal species *Lingulodinium machaerophorum* and *Spinifirerites bentorii* becoming more frequent during MIS 1 (although concentrations remain low, <118 and <784 cysts/g respectively). The occurrence of possible allochthonous coastal cysts in the open marine core record suggests that lateral transportation (or dissolution, as discussed below) might have affected the more recent assemblages. The continental shelf-slope topography in this region reveals a steep gradient, which makes offshore transportation extremely possible, especially during periods of high precipitation and river-runoff. However, a downcore analysis of clays from BAR9442, located ~50 km southwest of BAR-9403 but still on the continental slope offshore southern Sumatra identified minimal transportation effects on the clays (Gingele et al., 2002).

Unfortunately, as no neritic locations have been sampled for dinocysts near BAR-9403, it is not possible to confirm the relocation of cysts through comparative studies.

4.2.1.2. Reworking. Operculodinium janduchenei is regarded as an extinct species by McMinn et al. (2001), in contrast with Marret and Zonneveld (2003), who regarded it as extant, and provided global distribution maps in their atlas of modern species. This species is present in low concentrations irregularly throughout the core, but is also present in the most recent sample. It is regarded as extant herewith and, therefore, not indicative of reworking.

4.2.1.3. Selective decay and dissolution. Cyst degradation through oxidation can change the composition and absolute abundances of a fossil record (e.g. Esper and Zonneveld, 2007; Zonneveld et al., 1997, 2001; Versteegh and Zonneveld, 2002). Zonneveld et al. (1997) showed that cyst resistance to oxidation and degradation varied with genus and species. Protoperidiniacean species (eg, *Brigantedinium* spp.) were found to be the most susceptible, while *Nematosphaeropsis labyrinthus*, *Impagidinium* (e.g. *I. aculeatum, I. paradoxum* and *I. patulum*), *Operculodinium israelianum* and *Polysphaeridium zoharyi* the least.

The general correlation between peaks in concentrations of species sensitive and those resistant to aerobic decay (Figs. 6–7) suggests that selective dissolution has not biased the cyst assemblages throughout BAR-9403. This is also supported by foraminiferal evidence, with high accumulation rates of *U. proboscidea* during the 26–15 ka period.

Furthermore, very high concentrations of the moderately sensitive genus *Spiniferites* spp. (Esper and Zonneveld, 2007) from approximately 10.8 ka onwards are found to correlate with noticeably low peaks in the concentrations of the extremely sensitive species *Brigantedinium*, suggesting that any overprinting of the cyst signal caused by selective dissolution is minimal.

4.2.2. Climate-controlled changes in dinocyst assemblages

4.2.2.1. MIS 3 (up to 24 ka). Sea-surface productivity in the Java Upwelling System was reduced during MIS 3 and the early MIS 2 as the water column reached its maximum in stratification (Gingele et al., 2002). This regime would have effectively trapped nutrients in deeper water masses (Gingele et al., 2002). The absence of surface and sub-surface nutrients and increased predation/competition by copepods could effectively explain the low cyst concentrations (heterotrophic dominating over autotrophic species, with the H/A ratio consistently above 0.57) in BAR9403 during MIS 3 and the early MIS 2. Dinoflagellates were concluded to be outcompeted by copepods in sediment samples from the Banda Sea by van Waveren (1993) and van Waveren and Visscher (1994), who identified a predominance of heterotrophic species over autotrophic species in the majority of samples in the restricted upwelling regime.

The recent publication of Dürkop et al. (2008) covering the high resolution documentation of MIS3 for a core in the middle of the Timor Sea shows that the BFAR had similar values for those obtained for core BAR9403 [see Fig. 6e in Dürkop et al., 2008)]. In addition, changes of the BFAR in both cores can be related to sea-surface productivity/monsoon intensity variations, but we favour the scenario where increases in *B. aculeata* relate to reduced bottom water circulation instead. Increases of percentages of globocassidulids are related to changes in food sources (diatoms; according to Dürkop et al., 2008) consequent to an oceanic reorganisation. Such a feature was already suggested by Murgese and De Deckker (2007) for core Fr10-95/GC17 located offshore Northwest Cape except that the high percentages of *G. subglobosa* would have been related to a reduced food supply.

Interestingly, *O. centrocarpum* is consistently present during MIS 3, although in low concentrations. The ability of this species to adapt to unstable water columns (eg. the boundary zone between the neritic/oceanic regions and river plumes) is well documented in the literature, and has been used as an indicator of such environments (eg, Wall et al., 1977; Dale, 1996; Dale and Dale, 2002). The presence of *O. centrocarpum* during MIS 3 in low concentrations only suggests the well-stratified water column was an unsuitable environment for the production of this species.

Stelladinium robustum was found in the present study, although represented by only three specimens (at ~11 ka, 10.5 ka and 8.5 ka). This marks the first occurrence of this species in the Southern Hemisphere, as it was previously recorded only from shelf and open ocean locations within the Arabian Sea (Zonneveld et al., 1997; Zonneveld and Brummer, 2000). There, it was identified in mesotrophic to eutrophic environments with high summer temperatures (21.6 to 29.6 °C) and salinities (35.3 to 36.7), and with increased vertical mixing of the upper water column occurring during the Northeast Monsoon (Zonneveld, 1997). In addition, newly formed cysts were found during times of active upwelling in the Somalian upwelling area (Marret and Zonneveld, 2003).

4.2.2.2. MIS 2 (24 ka to 12 ka), with particular mention of the LGM (23 ka to 19 ka). Dinocyst concentrations do not show any notable variation at the onset of the LGM, although total species concentrations more than double from 674 cysts/g at 22.5 ka to 1585 cysts/g at 21.8 ka, indicating more favourable conditions for cyst development during this period. However, this change is temporary and the gradual but steady decline in total cyst concentrations after 21.8 ka until ~14.4 ka suggests that environmental conditions during and after the LGM (until 14.4 ka) remained largely unfavourable for overall cyst production. Total cyst concentrations generally decrease during this period from 957 cysts/g at 21.1 ka to 616 cysts/g at 15 ka. At the same time, the H/A ratio remained above 0.64 (bar two small troughs at 19.7 ka and 17 ka, when values fall marginally below 0.5 for the first time in the record). These data show that while there was no substantial increase in productivity during MIS 2, there were increasing periods of reduced productivity.

The only species to show increasing concentrations during this period of decreasing concentrations were *Impagidinium* spp. and *Spiniferites mirabilis*, both of which are predominantly oligotrophic, oceanic markers. The first occurrence of the predominantly oceanic genus *Impagidinium* in BAR9403 is at 19 ka and this species becomes consistently present in the core from 16.3 ka onwards until around 10.8 ka (bar an absence at 11.8 ka), although concentrations remain

low. *S. mirabilis* is more prominent in fully marine regions and while this species is present (in low concentrations) in the lower part of BAR9403, it becomes more dominant around 19.7 ka until ~10.8 ka. These species likely represent an allochthonous component of the cyst record.

Total cyst concentrations show a dramatic increase at ~14.4 ka, with both heterotrophic and autotrophic species concentrations nearly tripling previous values. This is likely associated with increased wind activity and precipitation, river runoff and nutrient supply with the onset of the monsoons favouring cyst production.

The consistent presence of *O. centrocarpum* after ~14.4 ka at slightly higher concentrations than previously seen could reflect decreasing stratification of the water column (e.g. increasing precipitation and/or monsoonal winds).

4.2.2.3. MIS 1 (12 ka to the present). As sea-surface temperatures (SST) and stratification of the upper water column increased during MIS 1, conditions became unfavourable for the continued relatively high concentrations of *O. centrocarpum* with the last occurrence this species in BAR9403 occurring at ~9.9 ka.

The sudden and extreme bloom of *Spiniferites* species during the Holocene is noteworthy, although reasons for such an occurrence are not known. *Spiniferites ramosus*, which makes up a large proportion of the autotrophic signature in BAR9403 during MIS 1, is a cosmopolitan species found in a wide variety of environments, although with highest abundances in mesotrophic to eutrophic regions characterized by upwelling or a well-mixed upper water column (Marret and Zonneveld, 2003). The peaks in concentration of *S. ramosus* do not correlate with any increases in heterotrophic species; in fact, the species indicative of increased productivity and/or upwelling (eg, *Brigantedinium*) displays low concentrations during this period. It is possible that the peak in *Spiniferites* species results from increased offshore transportation from the shelf due to increased precipitation, river runoff and sediment discharge at sea.

The coastal species *S. bentorii* becomes more common after 9.5 ka (although single specimens were recorded at 13.7 ka and 11.8 ka). However, concentrations remain >784 cysts/g at all other levels. Other coastal species (*Lingulodinium machaerophorum* and *Operculodinium israelianum*) are also more frequent from ~10.8 ka, although concentrations remain extremely low. The increasing presence – albeit minimal – of coastal species in core BAR9403 during MIS 1 represent increased relocation from shelf sediments down slope offshore Sumatra due to increased precipitation, river runoff and sediment discharge at sea.

Spiniferites delicatus is observed in minor amounts after 9.5 ka, although a single specimen was identified at 13.7 ka. Dale et al. (2002) identified a dominance of *S. delicatus* in samples from the outer plume of the Congo River, West-Central Africa, and suggested a relationship with an as yet unidentified type of nutrient enrichment, one distinct from the heterotrophic signal and one possibly derived from the land. This relationship was previously observed by Marret (1994) in the Gulf of Guinea, East Equatorial Atlantic Ocean, and by Marret et al. (1999) in the Congo Fan, West-Central Africa. Although concentrations of this species are low, the slight increase in *S. delicatus* in BAR9403 coincides with decreasing concentrations of heterotrophic species, with H/A ratios <0.22. While the low concentrations prevent interpretation of this species occurrence with confidence, it is likely that *S. delicatus* is also responding to increased river runoff and sediment discharge at sea.

The new species "*Spiniferites* 1," previously identified in three core top samples located near the Sunda Strait, where it reaches a peak relative abundance of 20% (Young, 2006), is only recorded at two horizons in the core (5.3 ka and the surface sample), and only three specimens in total are recorded. Further work in the region of Sumatra and the Sunda Strait is required to determine the exact nature of *S. delicatus* and "*Spiniferites* 1" in relation to possibly indicating nutrient enrichment that is different to that depicted by other heterotrophic species.

4.3. Evidence from benthic foraminifera

The benthic foraminifera species *O. t. umbonatus*, *E. exigua, B. aculeata* and *C. wuellerstorfi*, characterised the benthic foraminiferal fauna at different times during the last 35.7 kyr (see Fig. 10).

Oridorsalis tener umbonatus was the most abundant species until 26 ka BP (Fig. 10). At present, this species is related to a deep and cold environment, characterised by a low carbon-flux rate (Murgese and De Deckker, 2005). The percentage for this taxon, close to 30%, during this period, would indicate conditions of low productivity at the sea surface as also suggested by BFAR. Circulation offshore Java and Sumatra was different at that time: sea-surface currents, under the influence of strengthened Northwestern Monsoon (Gingele et al., 2002), and intermediate waters were characterised by a prevalent eastward flow. Under these conditions, the upwelling, which at Present is associated with the Southeastern Monsoon and the westward flow of the SJC, would have been suppressed or greatly reduced.

The isotopic signal (low $\delta^{13}C$ of *C. wuellerstorfi*) can then be attributed to enhanced stratification of the water column, which allowed the bloom of the giant diatom *Ethmodiscus rex* (De Deckker and Gingele, 2002; Gingele et al., 2002). The situation changed at 26 ka, when *O. t. umbonatus* was replaced by *B. aculeata*, which dominated the benthic foraminiferal assemblage between 26 and 14 ka, reaching percentages close to 50% (Fig. 10).

Analyses on Recent and living (stained) benthic foraminifera show a relationship between the abundance of *B. aculeata,* the sediment organic carbon content (Mackensen et al., 1993; Miao and Thunell, 1993; Rathburn and Corliss, 1994) and shallow oxygen penetration within the sediment (Miao and Thunell, 1996). The distribution of *B. aculeata* also correlates with high organic-carbon flux (>2 gC/m^2 yr) in the Atlantic and Southern Oceans (Altenbach et al., 1999). Similarly to *B. aculeata*, another species, *E. exigua*, showed increased percentage at this time. In the Eastern Indian Ocean, the distribution of this species outlines the preference for a deep environment, with pulsed fluxes of organic matter (Murgese and De Deckker, 2005). The high BFAR values would suggest an increased input of organic matter to the sea floor for this period. High carbon-flux rate is also suggested by the increased AR of *U. proboscidea*. This species would also indicate reduced oxygen levels (Murgese and De Deckker, 2005) and together with the low $\delta^{13}C$ of *C. wuellerstorfi*, would suggest a reduced deep-water circulation.

The *E. exigua* percentage peak suggests increased inputs of organic matter from the sea surface. The high *U. proboscidea* AR corroborates this hypothesis and indicates an enhanced flux of organic matter to the sea floor. As seen for the other cores, the *B. aculeata* bloom coincided with increased food supply and low-oxygen levels at the sea floor. The reduced percentage of *E. exigua* after 20 ka (Fig. 10) may be seen as the consequence of competition between these two species, which, in the presence of constant and significant amount of organic matter, would favour *B. aculeata*. This latter aspect can be related to the fact that in the presence of a high organic-matter oxidation-rate, oxygen depletion at the sea floor would occur.

Together with a reduction of deep-waters circulation, oxygen depletion could have played a major role in limiting *E. exigua*, thereby favouring *B. aculeata*. Low oxygen conditions are also suggested by the high value of dominance (D), which, during this period, reached the highest values recorded for the entire core. At the same time, the high percentage of infaunal taxa, which at Present are correlated with high carbon-flux rate and low-oxygen levels (Murgese and De Deckker, 2005), would support this hypothesis. Around 14 ka, *O. t. umbonatus* and *C. wuellerstorfi* became the most important species (Fig. 10). The environmental interpretation of these taxa has already been discussed, as together they would indicate a more oligotrophic environment characterised by intense bottom currents. Different factors

substantiate this interpretation: low *E. exigua* and *U. proboscidea* AR, the constant decrease of BFAR and the low percentage of infaunal taxa (indicating an environment more suitable for suspension feeders). The opening of the Sunda Strait, due to sea-level rise and the increased precipitation (Ganssen et al., 1988; van der Kaars and Dam, 1995), contributed to an injection of less saline water into the SJC path, inducing a low-salinity water cap, which reduced the effectiveness of the South Java Upwelling System (Martinez et al., 1999).

During the last 6 kyr, *B. aculeata* first and *E. exigua*, later, replaced the *O. t. umbonatus–C. wuellerstorfi* dominated assemblages. Again, this would suggest an increased food supply to the sea floor. However, the BFAR does not fully corroborate this interpretation, or at least points to a small increase compared to the one recorded for the past. This slight productivity variation at the sea surface can be associated with a reduced precipitation over the Australasian region during the last 6 kyr, compared to the period from 14 to 6 ka (van der Kaars and De Deckker, 2002). A similar event could have also taken place in this area, by reducing the low-salinity water cap importance over the South Java Upwelling System region and favouring a minimal primary productivity enhancement at the sea surface.

However, recent studies from the Arabian Sea found that the relationship between BFAR and organic carbon (C_{org}) is not valid for suboxic/dysoxic environments, where extremely low-oxygen levels can play a major role in controlling the population of benthic foraminifera by reducing the predation by macro-fauna (Naidu and Malmgren, 1995; den Dulk, 2000). The absence of parallel lamination in piston core BAR9403 does not support the idea of past reduced dissolved-oxygen concentrations comparable with those recorded for the Arabian Sea. Another factor that could undermine the reliability of BFAR is represented by the taphonomic processes affecting the benthic foraminiferal assemblage before its definitive burial, with the consequent loss of specimens in the fossil assemblage. Unfortunatel,y we did not carry out any sediment size analysis to determine possible factors such as sediment focussing that may provide additional information to support our hypothesis that a change in bottom circulation did occur during MIS2.

5. Conclusions

Below we provide in a chronological order a reconstruction of events that occurred in the Indian Ocean adjacent to the Island of Sumatra. This is based on all the proxies we have used in this study that relate to conditions at and near the sea surface and those that affected the sea floor around 2000 m water depth. We will proceed by always discussing conditions at the top of the water column first.

During MIS 3, there was an increase in DCM species (*N. dutertrei* and *N. pachyderma*) indicating stratified surface waters. In addition, there were abundant tropical species *P. obliquiloculata* which like warm waters and which lives higher in water column compared to *N. dutertrei*. Those species are indicative of separate temperature niches due to stratification. The extremely low total dinocyst concentrations (with the predominance of heterotrophic over autotrophic species) and the presence of copepod fragments identified in the fossil record during MIS 3 suggests cyst production was limited by an absence of surface and sub-surface nutrients and increased predation/competition. This is further confirmed by the benthic foraminifer fauna which also indicated oligotrophic conditions at the sea floor, thus implying no upwelling and a lack of organic carbon transport of the bottom.

During MIS 2, there was a clear stratification of the upper part of the water column but there was low nutrient availability due to relatively high percentage of tropical and subtropical oligotrophic species (*Gs. ruber* and *Gs. sacculifer*). According to the dinocyst flora, there is a small increase in dinocyst concentrations after the onset of the LGM, but the overall trend of gradually declining concentrations until approximately 14.4 ka suggests an environment that has remained largely unfavourable for successful dinocyst production (eg, low nutrient availability, high competition/predation). The benthic foraminifers imply an increase of the food supply to the sea floor, but it must not have come from above as there is no evidence for an increase of productivity at the sea surface as shown by dinoflagellates and planktic foraminifers, but more likely laterally as deep-sea circulation had slowed down.

During the MIS 2-1 transition, upwelling occurred, especially during the 14 to 9 ka interval as seen by a significant increase in the planktic foraminifers *Ga. bulloides* and *Gr. menardii*. The relatively high concentrations of the dinoflagellate *O. centrocarpum* between ~15–10 ka reflects a window of relative instability in the upper water column, as a result of the onset of the monsoonal system and associated winds, together with an increased precipitation and river runoff from Sumatra. This is interpreted from the significant increase in total dinocyst concentrations, especially autotrophic species. The benthic foraminifers provide a contrasting interpretation by indicating that, between 14 and 6 ka, oligotrophic conditions did occur at the sea floor. The only explanation for this discrepancy is perhaps seen but a reactivation of bottom circulation and that organic food supply was perhaps consumed before reaching the deep ocean. Around 11 ka, there was a clear stratification signal indicated by the increase of *N. dutertrei* and *N. pachyderma* similar to what was witnessed during MIS 3.

During MIS 1, oligotrophic tropical-subtropical conditions from 9 ka onwards are envisaged due to high relative abundances *Gs. ruber* and *Gs. sacculifer* and the stratification of the upper water column (due to the low salinity cap=barrier layer). Thus, conditions became unfavourable for the continued production of several planktonic foraminifer species. The dinocyst H/A ratio shows more variability from 10 ka onwards, although the gradual dominance of autotrophic species after that time indicates a change in the productivity signal to a more oligotrophic environment. The benthic foraminifers imply that between 6 and 2 ka there were seasonal pulses of organic matter to the sea floor and from 2 ka until today, oligotrophic conditions prevailed. The dinocysts further indicate that the extremely high abundances of the predominantly outer neritic genus *Spiniferites* during MIS 1 (especially after approximately 11.4 ka) is the result of increased offshore transportation from the continental shelf due to increased precipitation, river runoff and sediment discharge related to increasing monsoonal activity. The new species *Spiniferites* "1" is only present after ~8 ka and implies an environment experiencing high river runoff and sediment discharge, which supports the environmental preferences identified for this species in core tops from the eastern Indian Ocean (Young, 2006).

Acknowledgements

We are grateful to Dr F. Guichard (Gif-sur-Yvette) for making core BAR9403 available for this study. The core was obtained during the BARAT cruise in 1994 and the master and crew of the RV *Baruna Jaya* I are thanked for their effort. Scientists from MGI (Bandung), BPPT and LIPI (inJakarta) participated in the cruise which was partly funded by INSU (CNRS France), CEA, IFREMER and the 'service culturel' of the French Embassy in Jakarta. Operations at sea were performed with the help of Indonesian crew and 3 seamen from GENAVIR (IFREMER).

Stable isotopes were run by Joe Cali at the Research School of Earth Sciences at ANU and many of the samples prior to analysis were prepared by Mrs. Judith Shelley. Professor A. Altenbach provided advice to D. Murgese on benthic foraminifers. Funds for this project were provided to PDD by the Australian Research Council and we acknowledge the PhD stipends to D. Murgese [IPRS scholarship], M.I. Spooner [APA scholarship] and M. Young [ANU-RSPAS scholarship]. The AMS dates were performed at ANSTO by G. Jacobsen and her team and funded through AINSE grant 06/042 awarded to PDD. We are grateful for comments from Editor-in-Chief T. Corrège, S. van der Kaars and another anonymous reviewer. Their pertinent comments helped improve our manuscript.

References

Altenbach, A.V., Sarnthein, M., 1989. Productivity record in benthic foraminifera. In: Berger, W.H., Smetacek, V.S., Wefer, G. (Eds.), Productivity of the Ocean: Present and Past. John Wiley & Sons Limited, pp. 255–269. S. Bernhard, Dahlem Konferenzen.

Altenbach, A.V., Pflaumann, U., Ralph, S., Thies, A., Timm, S., Trauth, M., 1999. Scaling and distributional patterns of benthic foraminifera with flux rates of organic carbon. J. Foraminiferal Res. 29, 173–185.

Auras-Schudnagies, A., Kroon, D., Ganssen, G., Hemleben, C., Van Hinte, J.E., 1989. Distribution pattern of planktic foraminifers and pteropods in surface waters and top core sediments of the Red Sea, and adjacent areas controlled by the monsoonal regime and other ecological factors. Deep-Sea Res. 36 (10), 1515–1533.

Bard, E., 1998. Geochemical and geophysical implications of the radiocarbon calibration. Geochim. Cosmochim. Acta 62, 2025–2038.

Barmawidjaja, B.M., Rohling, E.J., van der Kaars, S., Vergnaud Grazzini, C., Zachariasse, W.J., 1993. Glacial condition in the Northern Molucca Sea region (Indonesia). Palaeogeogr. Palaeoclimat. Palaeoecol. 101, 147–167.

Bé, A.W.H., 1977. An ecological, zoogeographical and taxonomic review of Recent planktic foraminifera. In: Ramsay, A.T.S. (Ed.), Oceanic Micropaleontology, 1. Academic Press, London, pp. 1–100.

Bé, A.W.H., Hutson, W.H., 1977. Ecology of planktic foraminifera and biogeographic patterns of life and fossil assemblages in the Indian Ocean. Micropaleontology 23 (4), 369–414.

Bowman, G.M., 1985. Oceanic reservoir correction for marine radiocarbon dates from northwestern Australia. Aust. Archaeol. 20, 58–67.

Bray, N.A., Wijffels, S.E., Chong, J.C., Fieux, M., Hautala, S., Meyers, G., Morawitz, W.M.L., 1997. Characteristics of the Indo-Pacific Throughflow in the eastern Indian Ocean. Geophys. Res. Lett. 24, 2569–2572.

Cho, H.-J., Matsuoka, K., 2001. Distribution of dinoflagellate cysts in surface sediments from the Yellow Sea and East China Sea. Mar. Micropaleontol. 42 (3-4), 103–123.

Dale, B., 1996. Chapter 31. Dinoflagellate cyst ecology, modeling and geological applications. In: Jansonius, J.M., McGregor, D.C. (Eds.), Palynology: principles and applications. Am. Ass. Strat. Palynol. Found, vol. 3, pp. 1249–1275.

Dale, B., Fjellså, A., 1994. Dinoflagellate cysts as palaeoproductivity indicators: state of the art, potential and limits. In: Zahn, R., et al. (Ed.), Carbon cycling in the glacial ocean: constraints on the ocean's role in global change. Springer-Verlag, Berlin, pp. 521–537.

Dale, A.L., Dale, B., 2002. Appendix: application of ecologically based statistical treatment to micropalaeontology. In: Haslett, S.K. (Ed.), Quaternary Environmental Micropalaeontology. Arnold, London, pp. 259–286.

Dale, B., Dale, A.L., Jansen, F.J.H., 2002. Dinoflagellate cysts as environmental indicators in surface sediments from the Congo deep-sea fan and adjacent regions. Palaeogeogr. Palaeoclimat. Palaeoecol. 185, 309–338.

De Deckker, P., Gingele, F.X., 2002. On the occurrence of the giant diatom Ethmodiscus rex in a 80-ka record from a deep-sea core, southeast of Sumatra, Indonesia: implications for tropical palaeoceanography. Mar. Geol. 183, 31–43.

De Deckker, P., Tapper, N.J., van der Kaars, S., 2002. The status of the Indo-Pacific Warm Pool and adjacent land at the Last Glacial Maximum. Glob. Planet. Change 35, 25–35.

De Deckker, P., Yokoyama, Y. in press. Micropalaeontological evidence for Late Quaternary sea-level change in Bonaparte Gulf, Australia. Glob. Planet. Change.

den Dulk, M., 2000. Benthic foraminiferal response to Late Quaternary variations in surface water productivity and oxygenation in the northern Arabian Sea. Universiteit Utrecht, Utrecht. 205 pp.

de Vernal, A., Larouche, A., Richard, P., 1987. Evaluation of palynomorph concentration: do the aliquot and marker-grain methods yield comparable results? Pollen Spores 29 (2-3), 291–304.

Diester-Haass, L., Meyers, P.A., Vidal, L., 2002. The late Miocene onset of high productivity in the Benguela Current upwelling system as part of a global pattern. Mar. Geol. 180 (1-4), 87–103.

de Vernal, A., Guiot, J., Turon, J.L., 1993. Late and postglacial palaeoenvironments of the Gulf of St. Lawrence: marine and terrestrial palynological evidence. Géogr. Phys. Quat. 47 (2), 167–180.

Diester-Haass, L., Zahn, R., 2001. Paleoproductivity increase at the Eocene–Oligocene climatic transition: ODP/DSDP sites 763 and 592. Palaeogeogr. Palaeoclimat. Palaeoecol. 172 (1-2), 153–170.

Ding, X., Guichard, F., Bassinot, F., Labeyrie, L., Fang, N.Q., 2002. Evolution of heat transport pathways in the Indonesian Archipelago during last deglaciation. Chin. Sci. Bull. 47 (22), 1912–1917.

Ding, X., Bassinot, F., Guichard, F., Li, Q.Y., Fang, N.Q., Labeyrie, L., Xin, R.C., Adisaputra, M.K., Hardjawidjaksana, K., 2006. Distribution and ecology of planktic foraminifera from the seas around the Indonesian Archipelago. Mar. Micropaleontol. 58, 114–134.

Duplessy, J.-C., et al., 1984. $d^{13}C$ Record of benthic foraminifera in the last interglacial ocean: implications for the carbon cycle and the global deep water circulation. Quat. Res. 21 (2), 225–243.

Dürkop, A., Holbourn, A., Kuhnt, W., Zuraida, R., Andersen, N., Grootes, P., 2008. Centennial-scale climate variability in the Timor Sea during Marine Isotope 3. Mar. Micropaleontol. 66, 208–221.

Esper, O., Zonneveld, K.A.F., 2007. The potential of organic-walled dinoflagellate cysts for the reconstruction of past sea-surface conditions in the Southern Ocean. Mar. Micropaleontol. 65, 185–212.

Fairbanks, G.R., Wiebe, P.H., 1980. Foraminifera and chlorophyll maximum: vertical distribution, seasonal succession, and paleoceanographic significance. Science 209, 1524–1525.

Fink, D., Hotchkins, M., Hua, Q., Smith, A.M., Zoppi, U., Child, D., Mifsud, C., van der Gaast, H., 2004. The ANTARES AMS facility at ANSTO. Nucl. Instr. Meth. B 223–224, 109–115.

Ganssen, G.M., Kroon, D., 2000. The isotopic signature of planktic foraminifera from the NE Atlantic surface sediments: implications for the reconstruction of past oceanic conditions. J. Geol. Soc. 157, 693–699.

Ganssen, G., Troelstra, S.R., Faber, B., van Der Kaars, W.A., Situmorang, M., 1988. Late Quaternary paleoceanography of the Banda Sea, eastern Indonesian piston cores (Snellius-II expedition, cruise G5). Neth. J. Sea Res. 22, 491–494.

Gingele, F.X., De Deckker, P., Hillenbrand, C.-D., 2001. Late Quaternary fluctuations of the Leeuwin Current and palaeoclimates on the adjacent land masses — clay mineral evidence. Aust. J. Earth Sci. 48, 867–874.

Gingele, F.X., De Deckker, P., Girault, A., Guichard, F., 2002. High-resolution history of the South Java Current during the past 80 Ka. Palaeogeogr. Palaeoclimat. Palaeoecol. 183, 247–260.

Herguera, J.C., 2000. Last glacial paleoproductivity patterns in the eastern equatorial Pacific: benthic foraminifera records. Mar. Micropaleontol. 40, 259–275.

Herguera, J.C., Berger, W.H., 1991. Paleoproductivity from benthic foraminifera abundance: glacial to postglacial change in the West-Equatorial Pacific. Geology 19, 1173–1176.

Herguera, J.C., Berger, W.H., 1994. Glacial to postglacial drop in productivity in the western equatorial Pacific: mixing rate vs. nutrient concentrations. Geology 22, 629–632.

Hughen, K.A. and 26 other authors, 2004. Marine04 Marine Radiocarbon Age Radiocarbon. 46, 1059-1086.

Juggins, S., 2003. C2 User Guide 1.3. Software for ecological and palaeoecological data analysis and visualization. University of Newcastle, Newcastle-upon-Tyne, UK. 69 pp.

Kroon, D., Nederbragt, A.J., 1990. Ecology and palaeoecology of triserial foraminifera. Mar. Micropaleontol. 16, 25–38.

Levitus, S., 1998. World Ocean Atlas 1998. available at http://www.cdc.noaa.gov/.

Li, B.H., Jian, Z.M., Wang, P.X., 1997. Pulleniatina obliquiloculata as a paleoceanographic indicator in the southern Okinawa trough during the last 20,000 years. Mar. Micropaleontol. 32 (1-2), 59–69.

Linsley, B.K., Thunell, R.C., Morgan, C., Williams, D.F., 1985. Oxygen minimum expansion in the Sulu Sea, western equatorial Pacific, during the last glacial low stand of sea level. Mar. Micropaleontol. 9, 395–418.

Loubere, P., 1996. The surface ocean productivity and bottom water oxygen signals in deep water benthic foraminiferal assemblages. Mar. Micropaleontol. 28, 247–261.

Lutze, G.F., Thiel, H., 1988. Epibenthic foraminifera from elevated microhabitats: *Cibicidoides wuellerstorfi* and *Planulina ariminensis*. J. Foraminiferal Res. 19, 153–158.

Mackensen, A., Futterer, D.K., Grobe, H., Schmiedl, G., 1993. Benthic foraminiferal assemblages from the eastern South Atlantic Polar Front region between 35° and 57° S. Mar. Micropaleontol. 22, 33–69.

McMinn, A., Howard, W.R., Roberts, D., 2001. Late Pliocene dinoflagellate cyst and diatom analysis from a high resolution sequence in DSDP Site 594, Chatham Rise, south west Pacific. Mar. Micropaleontol. 43, 207–221.

Marret, F., 1994. Distributions of dinoflagellate cysts in Recent marine sediments from the East Equatorial Atlantic (Gulf of Guinea). Rev. Palaeobot. Palynol. 84, 1–22.

Marret, F., de Vernal, A., 1997. Dinoflagellate cyst distribution in surface sediments of the southern Indian Ocean. Mar. Micropaleontol. 29, 367–392.

Marret, F.Z., Zonneveld, K.A.F., 2003. Atlas of modern organic-walled dinoflagellate cyst distribution. Rev. Palaeobot. Palynol. 125, 1–200.

Marret, F., Scourse, J., Jansen, J.H.F., Schneider, R., 1999. Changements climatiques et paléocéanographiques en Afrique centrale atlantique au cours de la dernière déglaciation: contribution palynologique. Comptes rendus acad. sc.. Série II Fasc. A-Sc. terre et planètes, vol. 329, pp. 721–726.

Martinez, J.I., De Deckker, P., Barrows, T.T., 1999. Palaeoceanography of the last glacial maximum in the eastern Indian Ocean: planktic foraminiferal evidence. Palaeogeogr. Palaeoclimat. Palaeoecol. 147, 73–99.

Martinez, I.J., Taylor, L., De Deckker, P., Barrows, T.T., 1998. Planktic foraminifera from the eastern Indian Ocean: distribution and ecology in relation of the Western Pacific warm Pool (WPWP). Mar. Micropaleontol. 34, 121–151.

Martinson, D.G., Pisias, N.G., Hays, J.D., Imbrie, J., Moore, T.C., Shackleton, N.J., 1993. Age dating and the orbital theory of the ice ages: development of a high-resolution 0 to 300,000-year chronostratigraphy. Quat. Res. 27, 1–29.

Miao, Q.M., Thunell, R.C., 1993. Recent deep-sea benthic foraminiferal distributions in the South China and Sulu Seas. Mar. Micropaleontol. 22, 1–32.

Miao, Q.M., Thunell, R.C., 1996. Late Pleistocene–Holocene distribution of deep-sea benthic foraminifera in the South China sea and Sulu sea — palaeoceanographic implications. J. Foraminiferal Res. 26, 9–23.

Milliman, J.D., Farnsworth, K.L., Albertin, C.S., 1999. Flux and fate of fluvial sediments leaving large islands in the East Indies. J. Sea Res. 41, 97–110.

Müller, A., Opdyke, B.N., 2000. Glacial–interglacial changes in nutrient utilization and paleoproductivity in the Indonesian Throughflow sensitive Timor Trough, eastern-most Indian Ocean. Paleoceanography 15, 85–94.

Murgese, D.S., De Deckker, P., 2005. The distribution of deep-sea benthic foraminifera in core tops from the eastern Indian Ocean. Mar. Micropaleontol. 56, 25–49.

Murgese, S.D., De Deckker, P., 2007. The Late Quaternary evolution of water masses in the eastern Indian Ocean between Australia and Indonesia, based on benthic foraminifera faunal and carbon isotopes analyses. Palaeogeogr. Palaeoclimat. Palaeoecol. 247, 382–401.

Naidu, P.D., Malmgren, B., 1995. Do benthic foraminifer records represent a productivity index in oxygen minimum zone areas? An evaluation from the Oman Marin, Arabian Sea. Mar. Micropaleontol. 26, 49–55.

Paillard, D., Labeyrie, L., Yiou, P., 1996. Machintosh program performs time-series analysis. Eos. Trans. AGU 77, 379.

Pak, D.K., Kennett, J.P., 2002. A foraminiferal isotopic proxy for upper water mass stratification. J. Foraminiferal Res. 32 (3), 319–327.

Pflaumann, U., Jian, Z., 1999. Modern distribution patterns of planktic foraminifera in the South China Sea and western Pacific: a new transfer technique to estimate regional sea-surface temperatures. Mar. Geol. 156 (1), 41–83.

Rathburn, A.E., Corliss, B.H., 1994. The ecology of living (stained) deep-sea benthic foraminifera from the Sulu Sea. Paleoceanography 9, 87–150.
Rasmussen, T.L., Thomsen, E., Troelstra, S.R., Kuijpers, A., Prins, M.A., 2002. Millennial-scale glacial variability versus Holocene stability: changes in and benthic foraminifera faunas and ocean circulation in the North Atlantic during the last 60 000 years [Review]. Mar. Micropaleontol. 47 (1-2), 143–176.
Roncaglia, L., 2004. Palynofacies analysis and organic-walled dinoflagellate cysts as indicators of palaeo-hydrographic changes; an example from Holocene sediments in Skalafjord, Faroe Islands. Mar. Micropaleontol. 50 (1-2), 21–42.
Saito, T., Thompson, P.R., Berger, D., 1981. Systematic index of recent and Pleistocene Planktic foraminifera. University Press, Tokyo.
Southon, J., Kashgarian, M., Fontugne, M., Metivier, B., Yim, W.W.-S., 2002. Marine reservoir corrections for the Indian Ocean and Southeast Asia. Radiocarbon 44, 167–180.
Spooner, M.I., Barrows, T.T., De Deckker, P., Paterne, M., 2005. Palaeoceanography of the Banda Sea, and Late Pleistocene initiation of the Northwest Monsoon. Glob. Planet. Change 49 (1-2), 28–46.
Springtall, J., Tomczak, M., 1992. Evidence of the barrier layer in the surface layer of the tropics. J. Geophys. Res. 97, 7305–7316.
Sprintall, J., Wijffels, S., Chereskin, T., Bray, N., 2002. The JADE and WOCE I10/IR6 Throughflow sections in the southeast Indian Ocean. Part 2: velocity and transports. Deep-Sea Res. II 49, 1363–1389.
Struck, U., 1995. Stepwise postglacial migration of benthic foraminifera into the abyssal northeastern Norwegian sea. Mar. Micropaleontol. 26 (1-4), 207–213.
Stuiver, M., Polach, H., 1977. Reporting of 14C data. Radiocarbon 19, 355–363.
Stuiver, M., Reimer, P.J., and Reimer, R.W., 2006. CALIB 5.1. available at http://calib.qub.ac.uk/calib/.
Takahashi, K., Okada, H., 2000. The paleoceanography for the last 30,000 years in the southeastern Indian Ocean by means of calcareous nannofossils. Mar. Micropaleontol. 40, 83–103.
Thiede, J., Nees, S., Hartmut, S., De Deckker, P., 1997. Oceanic surface conditions recorded on the sea floor of the Southwest Pacific Ocean through the distribution of foraminifers and biogenic silica. Palaeogeog. Palaeoclimat. Palaeoecol. 131, 207–239.
Thomas, E., Booth, L., Maslin, M., Shackleton, N.J., 1995. Northeastern Atlantic benthic foraminifera during the last 45,000 tears — changes in productivity seen from the bottom up. Paleoceanography 10, 545–562.
Thompson, P.R., 1981. Planktic foraminifera in the Western Pacific during the past 150,000 years — comparison of modern and fossil assemblages. Palaeogeogr. Palaeoclimat. Palaeoecol. 35, 241–279.
Thunell, R.C., Reynolds, L.A., 1984. Sedimentation of planktic foraminifera: seasonal changes in species flux in the Panama basin. Micropalenotology 30, 243–262.
Thunell, R., Sautter, L.R., 1992. Planktonic foraminiferal faunal and stable isotopic indices of upwelling: a sediment trap study in the San Pedro Basin, Southern California Bight. In: Summerhayes, C.P., Prell, W.L., Emeis, K.C. (Eds.), Upwelling Systems: Evolution since the Early Miocene. Geological Society Special Publication, pp. 17–91.
van der Kaars, S., De Deckker, P., 2002. A Late Quaternary polen record from deep-sea core Fr10/95 GC17 offshore Cape Range Peninsula, northwestern Australia. Rev. Palaeobot. Palynol. 120, 17–39.
van der Kaars, W.A., Dam, M.A.C., 1995. A 135,000-year record of vegetational and climatic change from the Bandung area, West-Java, Indonesia. Palaeogeog. Palaeoclimatol. Palaeoecol. 117, 55–72.
van Waveren, I.M., 1993. Planktic organic matter in surficial sediments of the Banda Sea (Indonesia) — a palynological approach. Geologica Ultraiectina: Medel. Facult. Aardwetensch. Univ. Utrecht, vol. 104, pp. 1–237.
van Waveren, I.M., Visscher, H., 1994. Analysis of the composition and selective preservation of organic matter in surficial deep-sea sediments from a high-productivity area (Banda Sea, Indonesia). Palaeogeog. Palaeoclimatol. Palaeoecol. 112 (1-2), 85–111.
Versteegh, M., 1994. Recognition of cyclic and non-cyclic environmental changes in the Mediterranean Pliocene; a palynological approach. Mar. Micropaleontol. 23 (2), 147–183.
Versteegh, G.J.M., Zonneveld, K.A.F., 2002. Use of selective degradation to separate preservation from productivity. Geology 30 (7), 615–618.
Wall, D., Dale, B., Lochmann, G.P., Smith, W.K., 1977. The environmental and climatic distribution of dinoflagellate cysts in modern marine sediments from regions in the north and south Atlantic Oceans and adjacent seas. Mar. Micropaleontol. 2, 121–200.
Wang, L., Sarnthein, M., Erlenkeuser, H., Grimalt, J., Grootes, P., Heilig, S., Ivanova, E., Kienast, M., Pelejero, C., Pflaumann, U., 1999. East Asian monsoon during the Late Pleistocene: high-resolution sediment records from the South China Sea. Mar. Geol. 156, 245–284.
Wijffels, S.E., Bray, N., Hautala, S., Meyers, G., Werner, W.M.L., 1996. The WOCE Indonesian throughflow repeat hydrography sections: I10 and IR6. Int. WOCE Newsl. 24, 25–28.
Wyrtki, K., 1962. The upwelling in the region between Java and Australia during the south-east monsoon. Aust. J. Mar. Freshw. Res. 13, 217–225.
Yan, X.-H., Ho, C.-R., Zheng, Q., Klemas, V., 1992. Temperature and size variabilities of the Western Pacific warm pool. Science 258, 1643–1645.
Yokoyama, Y., Lambeck, K., De Deckker, P., Fifield, L.K., 2000. Timing of the Last Glacial Maximum from observed sea-level minima. Nature 406, 713–716.
Yokoyama, Y., De Deckker, P., Lambeck, K., Fifield, L.K., 2001. Sea-level at the Last Glacial Maximum: evidence from northwestern Australia to constrain ice volumes for oxygen isotope 2. Palaeogeogr. Palaeoclimat. Palaeoecol. 165, 281–297.
Young, M.D., 2006. The Distribution of Organic- and Calcareous-Walled Dinoflagellate Cysts from the Eastern Indian Ocean; A Proxy for Late Quaternary Palaeoceanographic Reconstructions. PhD thesis, Australian National University, Canberra, Australia. 342pp.
Zonneveld, K.A.F., 1997. New species of organic walled dinoflagellate cysts from modern sediments of the Arabian Sea (Indian Ocean). Rev. Palaeobot. Palynol. 97, 319–337.
Zonneveld, K.A.F., Brummer, G.-J.A., 2000. (Palaeo-)ecological significance, transport and preservation of organic-walled dinoflagellate cysts in the Somali Basin, NW Arabian Sea. Deep-Sea Res. II 47, 2229–2256.
Zonneveld, K.A.F., Versteegh, G.J.M., de Lange, G.J., 1997. Preservation of organic walled dinoflagellate cysts in different oxygen regimes: a 10 000 years natural experiment. Mar. Micropaleontol. 29, 393–405.
Zonneveld, K.A.F., Versteegh, G.J.M., de Lange, G.J., 2001. Palaeoproductivity and post-depositional aerobic organic matter decay reflected by dinoflagellate cyst assemblages of the Eastern Mediterranean S1 sapropel. Mar. Geol. 172, 181–195.